International Journal of Nanomedicine

Dovepress
open access to scientific and medical research

Open Access Full Text Article

ORIGINAL RESEARCH

# Tailoring of Retinyl Palmitate-Based Ethosomal Hydrogel as a Novel Nanoplatform for Acne Vulgaris Management: Fabrication, Optimization, and Clinical Evaluation Employing a Split-Face Comparative Study



Heba F Salem[1]
Rasha M Kharshoum[1]
Sara M Awad[2]
Mai Ahmed Mostafa[3]
Heba A Abou-Taleb[3]

[1]Department of Pharmaceutics and Industrial Pharmacy, Faculty of Pharmacy, Beni-Suef University, Beni-Suef, Egypt; [2]Department of Dermatology, Venereology and Andrology, Assiut University Hospital, Assiut, Egypt; [3]Department of Pharmaceutics and Industrial Pharmacy, Faculty of Pharmacy, Nahda University (NUB), Beni-Suef, Egypt

**Aim:** Retinyl palmitate (RP), the most stable vitamin A derivative, is used to treat photoaging and other skin disorders. The need to minimize the adverse effects of topical drug administration has led to an enhanced interest in loading RP on ethosomes for topical drug delivery. The aim of the current study was to prepare and compare the performance of RP decorated ethosomal hydrogel with tretinoin cream in the treatment of acne vulgaris as an approach to improve drug efficacy and decrease its side effects.

**Methods:** RP-loaded ethosomes were prepared using the injection sonication technique. A Box–Behnken design using Design Expert® software was used for the optimization of formulation variables. Particle size, zeta potential (ZP), entrapment efficiency percent (EE %), % drug release, and permeation over 24 h of different formulations were determined. The optimal formulation was incorporated into a hydrogel. Finally, the efficacy and tolerability of the optimized RP ethosomal hydrogel were clinically evaluated for acne treatment using a split-face comparative clinical study.

**Results:** The optimized ethosomal RP showed particle size of 195.8±5.45 nm, ZP of −62.1 ±2.85 mV, EE% of 92.63±4.33%, drug release % of 96.63±6.81%, and drug permeation % of 85.98 ±4.79%. Both the optimized RP ethosomal hydrogel and tretinoin effectively reduced all types of acne lesions (inflammatory, non-inflammatory, and total lesions). However, RP resulted in significantly lower non-inflammatory and total acne lesion count than the marketed tretinoin formulation. Besides, RP-loaded ethosomes showed significantly improved tolerability compared to marketed tretinoin with no or minimal skin irritation symptoms.

**Conclusion:** RP ethosomal hydrogel is considerably effective in controlling acne vulgaris with excellent skin tolerability. Therefore, it represents an interesting alternative to conventional marketed tretinoin formulation for topical acne treatment.

**Keywords:** ethosomes, Box–Behnken design, retinyl palmitate, topical delivery, acne vulgaris

## Introduction

Acne vulgaris is a chronic inflammatory disease of the skin affecting the pilosebaceous follicles. It commonly affects teenagers and young adults. It is characterized by dysregulated sebum production, disturbed follicular keratinization, Propionibacterium acnes colonization, inflammation, and immune responses.[1] Acne lesions can be subdivided into two major categories: inflammatory lesions, including papules, pustules,

Correspondence: Heba F Salem
Email heba_salem2004@yahoo.co.uk

Received: 26 January 2021
Accepted: 18 May 2021
Published: 24 June 2021

cysts, nodules; and non-inflammatory lesions (comedones).[2,3] Treatment strategies are based on minimizing keratinocyte hyperproliferation, seborrhea, colonization by Propionibacterium acnes, and inflammation. Topical treatment, especially topical retinoids, is the first choice in mild to moderate acne, whereas systemic therapy is used for treating moderate to severe cases.[4]

International treatment guidelines emphasize the key role of topical retinoids in acne management.[5–7] Topical retinoids exert pleiotropic effects on acne; they normalize follicular keratinocyte proliferation and regulate follicular epithelial turnover, which helps extrusion of comedones and inhibit microcomedone formation.[8] Moreover, they have antimicrobial activity against the Propionibacterium acnes.[9–12] Besides, topical retinoids have anti-inflammatory properties by modulating the inflammatory mediators and inflammatory cell migration.[13]

Although highly effective in treating acne, the use of retinoic acid topically is frequently accompanied by a high incidence of side effects as sunlight sensitivity, peeling, burning, pruritus, and erythema.[14] These cutaneous reactions tend to reduce patient compliance and compromise therapy.[10,14] Some retinoid derivatives, such as tretinoin, isotretinoin, tazarotene, and adapalene were developed to overcome these problems. However, they still cause local cutaneous irritation in a considerable number of patients.[15] Several approaches have been proposed to reduce these side effects, including the use of nanosystems for targeted topical delivery of retinoids and the use of esters of retinoic acid as retinyl palmitate (RP).[14,16,17]

RP is the most stable form of retinoic acid,[18] commonly used as anti-aging due to its effectiveness at regulating epithelial cell growth and differentiation and boosting collagen production. Experimental studies have emphasized the valuable role of RP in increasing skin elasticity, decreasing skin roughness, and preventing the peroxidation of skin lipids.[3,19,20] It also enhances the appearance of the skin and reduces keratosis in sun-damaged skin.[9,10]

The inclusion of RP into nanocarriers for topical treatment of acne is an exciting strategy that can lead to higher stability and enhance skin penetration. Ethosomes are soft phospholipid nanovesicles used for enhanced dermal and transdermal delivery of drugs.[21,22] They contain a high ethanol concentration, which improves skin permeation[21–24] as it acts as a penetration enhancer. It penetrates intercellular lipids, increases lipid fluidity, and decreases the density of lipid multilayer of the cell membrane,[23,24] which increases skin permeability. Therefore, ethosomes permeate easily into the deep skin layers and fuse with skin lipids, leading to drug release in deep skin layers.[23,24]

This study aimed to develop the ethosomal gel of RP to overcome side effects caused by conventional retinoids and improve penetration and localization of drugs into deep skin layers. The physicochemical characteristics of RP ethosomal formulation were assessed. Clinical evaluation of the efficacy and tolerability of patients suffering from mild to moderate facial acne vulgaris was carried out compared to tretinoin cream.

# Materials and Methods

## Materials

Retinyl Palmitate (RP) was purchased from Labeyond Chemicals Co., (Ltd., Dalian, China). Phosphatidylcholine (PC) and ethanol (High-performance liquid chromatography-grade) were purchased from Sigma- Aldrich (St. Louis, MO, U.S.A.). Propylene glycol (PG) was provided as a gift by C.I.D. Pharmaceutical (Assiut, Egypt). Carbopol 971P, Chitosan, and Dimethyl Sulfoxide (DMSO) were purchased from El-Nasr Pharmaceutical Chemical Company (Cairo, Egypt). All other materials and solvents were of high analytical grade.

## Experimental Design

A Box–Behnken design generated with Design Expert® (Version 10, Stat-Ease Inc. Minneapolis, MN) was used to prepare fifteen formulations of ethosomal RP where the independent variables were the concentrations of PC (A), ethanol (B), and PG (C). The dependent variables were particle size ($Y_1$), zeta potential ($Y_2$), entrapment efficiency (EE%) ($Y_3$), % of RP released from ethosomes after 24 h ($Y_4$), and % of RP permeated from ethosomes after 24h ($Y_5$) as shown in (Table 1).

## Preparation of Ethosomal RP Formulations

RP ethosomes were prepared using an injection sonication technique.[25] In brief, a proper amount of RP (5 mg) was weighed, and various concentrations of PC were dissolved along with various concentrations of alcoholic phase (ethanol and PG). Each mixture was continuously agitated and tightly closed in a sealed container to avoid ethanol evaporation. Next, freshly prepared deionized water (aqueous phase) was added using a syringe system to the alcoholic phase dropwise at 30±2°C. The dispersed vesicles were exposed to sonication and then stored for further investigation at 4°C.

**Table 1** Composition of the Independent Variables with Their Respective Levels and Their Dependent Variables

| **Variables** | **Levels** | | | | | | | | |
|---|---|---|---|---|---|---|---|---|---|
| Independent variables (Factors) | Low(−1) | | | Medium(0) | | | High(+1) | | |
| A = PC concentration % (w/v) | 1% | | | 2% | | | 3% | | |
| B = Ethanol concentration % (v/v) | 10% | | | 20% | | | 30% | | |
| C = PG concentration % (v/v) | 5% | | | 10% | | | 15% | | |
| Formula no. | Independent variables | | | Dependent variables | | | | | PDI |
| | A | B | C | Y1: particle size (nm) | Y2: zeta potential(mV) | Y3:EE% | Y4: % drug released over 24h | Y5: % drug permeated over 24h | |
| F1 | +1 | +1 | 0 | 354.3±9.36 | −77.5±3.99 | 98.86±5.01 | 83.69±8.29 | 74.26±5.92 | 0.46 |
| F2 | 0 | −1 | −1 | 340±4.35 | −61.1±4.32 | 89.23±4.88 | 67.2±6.38 | 55.16±5.28 | 0.43 |
| F3 | 0 | 0 | 0 | 271.4±6.48 | −59.5±4.28 | 93.81±3.74 | 76.73±4.41 | 73.5±6.99 | 0.35 |
| F4 | 0 | −1 | +1 | 311±8.27 | −54.5±7.84 | 92.76±6.55 | 73.23 ±11.01 | 61.38±3.09 | 0.30 |
| F5 | −1 | +1 | 0 | 174.5±5.36 | −56.1±2.09 | 91.24±7.98 | 97.9±3.92 | 85.18±5.61 | 0.26 |
| F6 | +1 | −1 | 0 | 404±10.43 | −66.3±5.82 | 95.84±4.72 | 62.48±8.54 | 51.53±4.33 | 0.36 |
| F7 | +1 | 0 | +1 | 367.6±13.49 | −72.6±9.75 | 98.27±3.91 | 75.4±4.09 | 63.28±4.72 | 0.37 |
| F8 | −1 | −1 | 0 | 310.1±3.52 | −51±8.35 | 82.01±6.02 | 79.87±2.74 | 68.38±9.51 | 0.39 |
| F9 | +1 | 0 | −1 | 386.4±5.33 | −74.2±3.17 | 97.97±7.53 | 70.43 ±10.61 | 58.83±6.42 | 0.34 |
| F10 | 0 | 0 | 0 | 283.5±6.63 | −62±5.29 | 95.09 ±11.23 | 78.83±6.81 | 68.87±3.99 | 0.46 |
| F11 | 0 | +1 | +1 | 237.4±3.81 | −67±10.56 | 96.39±2.84 | 93.87±8.49 | 83.28±5.91 | 0.33 |
| F12 | 0 | +1 | −1 | 261.3±2.69 | −72.6±3.88 | 96.03±3.52 | 87.9±7.90 | 76.94±8.53 | 0.36 |
| F13 | −1 | 0 | −1 | 228.4±11.51 | −52.3±3.11 | 84.12±9.19 | 82.24 ±14.73 | 72.38±7.28 | 0.32 |
| F14 | −1 | 0 | +1 | 199.4±3.33 | −58.2±4.02 | 87.13±4.92 | 89.24±5.44 | 78.53±4.74 | 0.26 |
| F15 | 0 | 0 | 0 | 293.6±9.46 | −60.6±6.53 | 93.91±3.06 | 75.49±5.38 | 71.32±5.26 | 0.21 |
| F optimized | 1.33% | 30% | 15% | 195.8±5.45 | −62.1±2.85 | 92.63±4.33 | 96.63±6.81 | 85.98±4.79 | 0.37 |

**Note**: Data are mean values (n = 3) ± SD.
**Abbreviations**: PC, Phosphatidyl choline; PG, Propylene glycol; EE%, entrapment efficiency percent; PDI, polydispersity index.

## Characterization of Ethosomal RP Formulations

### Determination of Particle Size and Zeta Potential

The average particle size and ZP of ethosomal RP were determined by the dynamic light scattering method (DLS) using a Malvern Mastersizer (Malvern Instruments GmbH, Herrenberg, Germany). Dilution of each dispersion and measurement in triplicate were performed at 25±1°C.[26–28]

### Determination of Entrapment Efficiency (EE%)

Determination of EE% of the ethosomal suspension was carried out by applying ultracentrifugation technique using

a cooling centrifuge (SIGMA 3–30K, Steinheim Germany) at 14,000 rpm, for 3 h at 4°C.[29] The supernatant (containing free RP) was separated from the sediment (ethosomal pellets), diluted with distilled water, and finally analyzed using a UV spectrophotometer (Shimadzu UV-1800, Tokyo, Japan) at $\lambda_{max}$ of 325 nm. The following equation was used to calculate EE% for all formulations:[30,31]

$$EE\,\% = \frac{\text{Weight of total RP} - \text{Weight of free RP}}{\text{Weight of total RP}} X\,100 \quad (1)$$

### In-vitro Drug Release Study

The in-vitro release of ethosomal RP was performed and compared to free RP suspension by the dialysis method using USP I dissolution apparatus (Erweka DT-720, Erweka GmbH, Heusenstamm, Germany).[29] According to the calculated EE%, accurate volumes of ethosomal RP (equivalent to 3 mg of RP) were added to glass cylinders (6 cm length and 2.5 cm internal diameter) tightly covered with the dialysis membrane, which was soaked in the receptor medium overnight from one end. The cylinders were fixed at the U.S.P. dissolution tester apparatus shafts. The release medium was filled with 100 mL Sörensen's phosphate buffer pH 5.5 containing 1% tween 20 and kept at 37± 0.5°C with continuous stirring at 100 rpm.[32] At determined intervals (1, 2, 3, 4, 6, 8, 10, 12, and 24 h), a sample of 2 mL from the receptor compartment was withdrawn, and an equal volume of fresh media was substituted to keep a constant volume. A filter of 0.45 µm Millipore was used to filter the withdrawn samples and then analyzed by the UV method, as mentioned previously. The in-vitro release pattern of the free RP suspension in distilled water was also investigated in the same way. The percent of RP released was calculated for all ethosomes using the following equation:[33]

$$\%\ of\ Rreleased = \frac{The\ amount\ of\ RP\ at\ time\ t}{Total\ amount\ of\ RP} \times 100 \quad (2)$$

The release data was used to determine the release pattern using different release kinetic models as zero order, first order, and Higuchi's matrix.[34]

### Ex-vivo Permeability Study

The permeability study was conducted in line with the Animal Ethical Guidelines for Investigations in Laboratory Animals and was approved by the Ethical Review Board of Faculty of Pharmacy, Minia University, Egypt (Ref: 66/2019). Wistar rats (6–8 weeks old, 100–125 g) under anesthesia were euthanized using decapitation, and each rat's dorsal skin was excised. The hair on animals' skin was stripped via shaving, and the skin was washed with distilled water. Prepared skin was then mounted on the diffusion cells where the skin dermal side faced the receptor medium, and the SC side faced the donor compartment.

Franz diffusion cell of 5 $cm^2$ surface area was used for ex-vivo diffusion studies. The receptor chamber was filled with 100 mL phosphate buffer saline pH 6.4 containing 1% tween 20 as diffusion medium, which was maintained at 32 ± 0.5°C and stirred at 100 rpm. Different ethosomal RP holding constant quantities of RP (3 mg) were added to the donor compartment. Samples from the receptor compartment were withdrawn at determined time intervals (1, 2, 3, 4, 6, 8, 10, 12, and 24 h) then equal volumes of fresh milieu were added to the receptor chamber. A filter of a 0.45 µm Millipore was used to filter the withdrawn samples and then measured at 325 nm using a spectrophotometer. The following equation was used for calculating the % of RP permeated:

$$\%\ \text{of RP permeated} = \frac{\text{The amount of RP at time t}}{\text{The total amount of RP}}\ X\,100 \quad (3)$$

For permeation parameters calculation, the cumulative permeated amount of RP per unit area (µg/$cm^2$) was plotted against time (h) for all formulations. Steady-state flux (Jss) in µg/$cm^2$ h and permeability coefficient (Kp) in cm/h were calculated for each ethosomal RP formulation to evaluate the improvement in the RP permeation in comparison to the RP suspension (control). The lag time, which is the time of the drug to start permeation, was determined from the x-axis intercept (the linear portion of the graph).

## Optimization of Ethosomal RP Formulations

To select the optimum ethosomal formulation Design-Expert® software was by applying the desirability function. The optimization process was designed to get the least PS formulation with the highest EE%, % RP released and permeated after 24 h and ZP as an absolute value in range. The solution with a desirability factor near to one was selected. The selected formulation was prepared, characterized, and compared with the predicted responses to verify the model's efficacy.

## Morphology of the Optimized Ethosomal RP Formulation

Transmission electron microscope (TEM-HR-2100, Joel, JAPAN) was used to examine the morphology of the

optimized ethosomal RP formulation at an accelerating voltage of 80 K.V. The freshly prepared diluted sample was negatively stained with 1% w/v phosphotungstic acid then applied onto the carbon-coated grid and was left to dry at room temperature to allow the adherence of vesicles to the carbon grid.[35]

## Physical Stability

Physical stability of the optimal ethosomal RP formulation was evaluated by examining changes of mean particle size, ZP, and EE% during storage at 4°C and 25°C protected from the light for 90 days.[12,36,37]

## Preparation of RP Ethosomal Hydrogel

### Experimental Design

The optimized ethosomal RP hydrogel was prepared using the Historical Data Design Expert® (Version 10, Stat-Ease Inc. Minneapolis, MN) to study the relationship between independent and dependent variables (Table 2).

### Fabrication Method

Various concentrations of different polymers (cationic polymer Chitosan as well as the anionic polymer Carbopol 971P) and various concentrations (1% and 2%) of permeation enhancer (DMSO) were used in hydrogel matrices preparation. In the required quantity of distilled water, different hydrogel bases and DMSO were added and solubilized. The optimized ethosomal RP formulation was then added to the polymer solution with continuous Stirring using a mechanical stirrer at 500–1000 rpm until the uniform solution was obtained. The final preparation was kept at 5°C for about 10–12 h to ensure the complete dissolving of polymers in the solution. The final concentration of RP was 0.5 mg/g in all preparations. Drops of 0.1N acetic acid were needed to dissolve chitosan, while a drop of 10% triethanolamine solution was needed for Carbopol 971P containing hydrogels to achieve clarity. Carbopol 971P, chitosan, and DMSO were added in concentrations outlined in the experimental design portrayed by the design expert (Table 2).[38]

### In-vitro Characterization of RP Ethosomal Hydrogel

#### Rheological Characterization of Ethosomal Hydrogel Formulations

The rheological properties of the ethosomal hydrogel formulations were obtained using Brookfield viscometer (DV-III Ultra viscometer, R.V. model, Brookfield, U.S. A.). The measurements were performed at 25±1°C using spindle 52 connected to the viscometer by a circulating bath at a shear rate varying from 20 to 200 ($sec^{-1}$).[39] The viscosities, and the area of hysteresis loops, were assessed. Farrow's equation was used to determine the flow behavior of hydrogel bases:

$$\log G = N \log F - \log \eta \quad (4)$$

where G is the shear rate ($sec^{-1}$), F is the shear stress ($dyne/cm^2$), η is the viscosity (cP), and N is the constant of Farrow, which indicates the deviation from Newtonian law. When N is less than one, dilatant flow (shear rate thickening) is suggested. However, if N is greater than one, the flow will be plastic or pseudoplastic (shear rate thinning).

#### In-vitro Drug Release Study

The in-vitro release profiles of RP hydrogel were performed and compared to RP suspension in a USP I dissolution apparatus adopting the dialysis bag diffusion method as described before.

#### Ex-vivo Permeability Study

Permeability studies of RP ethosomal hydrogel formulations were performed and compared to RP suspension as described above in the ex-vivo permeability study using Franz diffusion cell.

#### Optimization of RP Ethosomal Hydrogel

The optimization process was designed to get a formulation with the highest % RP released and % RP permeated after 24h.

### Skin Irritation Studies

#### Animals

An 18 female Wistar rats weighing 150–200 g obtained from the animal facility of Minia University (Minia, Egypt) were divided randomly into 3 groups (normal control, ethosomal RP hydrogel treated, and tretinoin cream treated) and housed in polyacrylic cages (six animals per cage). All animals were fed with normal chow and tap water ad libitum. An adequate amount of gel and cream were applied on rats' dorsal side once a day for five consecutive days per week, for two weeks after shaving the hairs. For treatment safety evaluation, the incidence of adverse effects as skin irritation and erythema was observed at the application site of rats throughout treatment. Rats were sacrificed by cervical decapitation under anesthesia at the end of the study. The application area and non-application area (served as a control) of the same

**Table 2** Formulation Parameters for RP Ethosomal Hydrogel

| Independent Variables | Levels | | | | Dependent Variables | | | | Constraint |
|---|---|---|---|---|---|---|---|---|---|
| | 0 | | 1 | | | | | | |
| Polymer type ($X_1$) | Carbopol 971P | | Chitosan | | % RP released from ethosomal hydrogel | | | | Maximum |
| Polymer conc. ($X_2$) | 1 | | 2 | | % RP permeated from ethosomal hydrogel | | | | Maximum |
| Surfactant (DMSO) conc. ($X_3$) | 1 | | 2 | | | | | | |
| Formulation | G1 | G2 | G3 | G4 | G5 | G6 | G7 | G8 | $G_{optimized}$ |
| Polymer type ($X_1$) | 0 | 0 | 0 | 0 | 1 | 1 | 1 | 1 | 0 |
| Polymer conc. ($X_2$) | 1 | 1 | 2 | 2 | 1 | 1 | 2 | 2 | 1 |
| Surfactant conc. ($X_3$) | 1 | 2 | 1 | 2 | 1 | 2 | 1 | 2 | 2 |
| % drug released ($Y_1$) | 84.83± 2.33 | 89.39± 3.84 | 72.61± 7.63 | 77.99± 4.92 | 63.97± 9.16 | 65.94± 3.94 | 53.54± 4.81 | 59.16± 4.02 | 86.75± 5.82 |
| % drug permeated ($Y_2$) | 72.96± 8.83 | 75.47± 3.80 | 58.97± 1.42 | 65.64± 0.34 | 42.58± 3.92 | 49.99± 4.55 | 38.25± 5.12 | 41.36± 3.68 | 75.89± 3.88 |
| Viscosity (cP) | 5448.64 | 4768.96 | 6405.12 | 6029.28 | 1351.84 | 1272.32 | 2067.52 | 1431 | 4798.34 |
| Farrow's constant (N) | 5.281 | 3.507 | 4.478 | 3.42 | 2.272 | 1.5 | 1.779 | 3.453 | 3.550 |
| Area of hysteresis loop (Dyne/$cm^2$.sec) | 1527.36 | 2035.71 | 667.96 | 1953.12 | 683.87 | 858.81 | 763.39 | 1304.05 | 2835.288 |

**Note**: Data are mean values (n = 3) ± SD.
**Abbreviations**: DMSO, Dimethyl Sulfoxide; RP, Retinyl Palmitate.

animal were removed, rinsed with normal saline, and preserved in 10% neutral buffered formalin for histopathological investigation. This study was approved by "The Commission on the Ethics of Scientific Research," Faculty of Pharmacy, Minia University.

### Histological Examination

Skin specimens of three rats of each group were collected randomly. Tissues were perfused with normal saline and preserved in 10% neutral phosphate-buffered formalin, and embedded in paraffin. The prepared section was then deparaffinized using xylol and consequently hydrated in ethyl alcohol. After dehydration, paraffin-embedded tissue sections (5 μm) were stained with hematoxylin and eosin (H&E) according to the method of Bancroft & Gamble.[40] Sections were photographed using a digital camera attached to a light microscope.

## Clinical Evaluation of the Optimized RP Ethosomal Hydrogel

### Patients

The study was carried out on 20 patients with facial acne vulgaris (18 females and 2 males), recruited from the Dermatology Outpatient Clinic, Assiut University Hospital, Assiut, Egypt, between September 2019 and December 2019.

The clinical study excluded patients taking other concomitant oral and topical acne medication, chemical peeling or light-based acne treatment during the study course, pregnant females, and patients with facial skin problems such as rosacea, perioral dermatitis, or atopic dermatitis. The study included patients above 18 years old with mild to moderate facial acne vulgaris. The baseline acne severity was graded using the Comprehensive Acne Severity Scale.[41] This scale consists of three categories: Mild acne: number of comedones less than 20 inflammatory lesions less than 15 or a total count of lesion less than 30. Moderate acne: Number of comedones 20–100, or inflammatory lesions 15–50, or a total count of the lesion is 30–125. Severe acne: number of cysts higher than 5, or count of comedones higher than 100, or a total inflammatory count higher than 50, or a total count of the lesion is higher than 125. This study was conducted in compliance with the guidelines of the Declaration of Helsinki, and the Research Ethics Committee of the Faculty of Medicine, Assiut University approved the study protocol (I.R.B. no. 17300308). Informed consent was obtained from all patients before enrolment as well as for the images to be published. Also, the authors do not intend to share individual de-identified participant data. The protocol of the study was also registered at Clinical Trials.gov (ID: NCT04080869).

### Study Design and Treatment Protocol

A prospective, split-face comparative clinical study was conducted. All patients were assigned to apply a thin film of topical tretinoin cream (AcretinTM® 0.05%, Jamjoom Pharma, Egypt) on the right side of the face and the optimized ethosomal RP hydrogel (0.05%) on the left side of the face every night for 6 weeks. Before topical treatment was applied, the face was washed using a non-abrasive cleanser, with care to avoid the eyes and lips. The two topical products were packed in biweekly batches of 15 g, in non-identifiable jars by a nurse who was not involved in the study.

### Evaluation

Patients were assessed before starting treatment (baseline) and at 2, 4, and 6 weeks. Digital photographs were taken at baseline, at each visit, and at the end of the treatment (after 6 weeks) using identical camera settings (Nikon, Coolpix L330, 20.2 megapixels, 26x zoom Nikkor, China). Medication efficacy was determined by counting lesions on both sides of the face, which was carried out by a blinded and trained dermatologist. The patients were assessed for any change from the baseline in the number of non-inflammatory lesions (open and closed comedones), the number of inflammatory lesions (papules, pustules, and nodules), and the number of overall lesions at each visit (0, 2, 4, and 6 weeks). For the final assessment, the number of lesions counted in the first visit is considered to be 100%, and any decrease in the number of lesions is calculated accordingly and regarded as a percentage reduction to determine the treatment efficacy. The assessment of tolerability was done by interviewing the patients about any adverse reactions (erythema, peeling, burning sensation, and pruritus) at each visit on a 4-point scale as 0; no adverse event reported; 1, mild; 2, moderate; or 3, severe adverse event(s). During the trial, the patients were instructed to avoid using any other anti-acne treatments.

### Statistical Analysis

Statistical analysis was performed using SPSS software version 18.0 (SPSS Inc., Chicago, IL, U.S.A.). Data were presented as mean± SD or frequencies and percentages. Comparing the differences between before and after

treatment and those between the two treatment sides, paired *t*-test or Wilcoxon signed-rank test and the Chi-square test were used. P-value < 0.05 is considered statistically significant.

# Results and Discussion

## Experimental Design and Data Analysis

Design-Expert® software was used for statistical analysis of the data obtained using a Box–Behnken design. Based on preliminary experiments on the viability of preparing ethosomal RP, the three factors with three levels of each of the three factors were chosen (PC, ethanol, and propylene glycol). The signal-to-noise ratio was measured accurately to ensure that the model could be used to navigate the design space.[42,43] All parameters (EE%, particle size, ZP, % of RP released from ethosomes after 24 h, and % of RP permeated from ethosomes after 24 h) have a ratio >4, which is desirable. The adjusted and predicted $R^2$ values should be close to each other in fair agreement,[44] which has been achieved for all parameters (Table 3). The experimental run and the measured parameters are listed (Table 1).

## The Particle Size of Ethosomal RP Formulations

Forming vesicles with optimum particle size is essential to enhance ethosomal RP passage through the skin. As depicted in (Table 1), the mean vesicle size of the ethosomes fluctuated from 174.5±5.36 to 404±10.43 nm with P.D.I. ranges from 0.21 to 0.46. The effect of the PC concentration (A), the concentration of ethanol (B), and the concentration of PG (C) on the particle size of the ethosomes are illustrated graphically as 3-D surface plots in (Figure 1A). ANOVA showed a significant effect for the concentration of PC (A) and ethanol concentration (B) (P=0.0001) on PS, while the effect of the concentration of PG (C) was not significant (P=0.09828). The ethosomal particle size increased with increasing the concentration of PC Phospholipids are the main component of the ethosomal wall and therefore expected to increase wall thickness and therefore increase particle size.[45] It is worth noting that propylene glycol and ethanol concentration had an antagonistic effect on the mean ethosomes' size;[46,47] this can be interpreted to the negative charge gained by both ethanol and PG, which causes electrostatic repulsion and prevention of vesicle aggregation.[48]

Furthermore, the reduction in membrane thickness resulted from the interaction of ethanol and PG with the lipid bilayer.[47,49] The decreased PS at higher concentration of ethanol from (10–30%) may be due to ethanol interaction with the lipid bilayer, which causes PS of the vesicles to decrease.[50–53] Salem et al observed similar results working on Lercanidipine HCl nano-ethosomal gel.[54]

**Table 3** Summarize Statistics Model of Box–Behnken Design Used for Optimization of Ethosomal RP with Their Regression Equation

| Dependent Variables | $R^2$ | Adjusted $R^2$ | Predicted $R^2$ | P value |
|---|---|---|---|---|
| $Y_1$: particle size(nm) | 0.9341 | 0.9161 | 0.8692 | 0.0001 |
| $Y_2$: ZP (mV) | 0.9032 | 0.8768 | 0.8127 | 0.0001 |
| $Y_3$: % EE | 0.9918 | 0.9772 | 0.9070 | 0.0001 |
| $Y_4$: % drug released over 24 hr | 0.9658 | 0.9564 | 0.9462 | 0.0001 |
| $Y_5$: % drug permeated over 24 hr | 0.9715 | 0.9638 | 0.9532 | 0.0001 |
| Regression equation of the fitted model | | | | |
| $Y_1$= 294.86 + 74.9875A - 42.2 B - 12.5875C | | | | |
| $Y_2$= 63.0333 + 9.125A + 5.0375 B - 0.9875 C | | | | |
| $Y_3$= 94.27 + 5.805 A+ 2.835B + 0.9C- 1.5525AB - 0.6775AC - 0.7925 BC- 2.00625 $A^2$–0.27625 $B^2$ –0.39125 $C^2$ | | | | |
| $Y_4$= 79.6333–7.15625A + 10.0725B + 2.99625 C | | | | |
| $Y_5$= 69.5213–7.07125A + 10.4013B + 2.895 C | | | | |

**Note**: Data are mean values (n = 3) ± SD.
**Abbreviation**: EE%, entrapment efficiency percent.

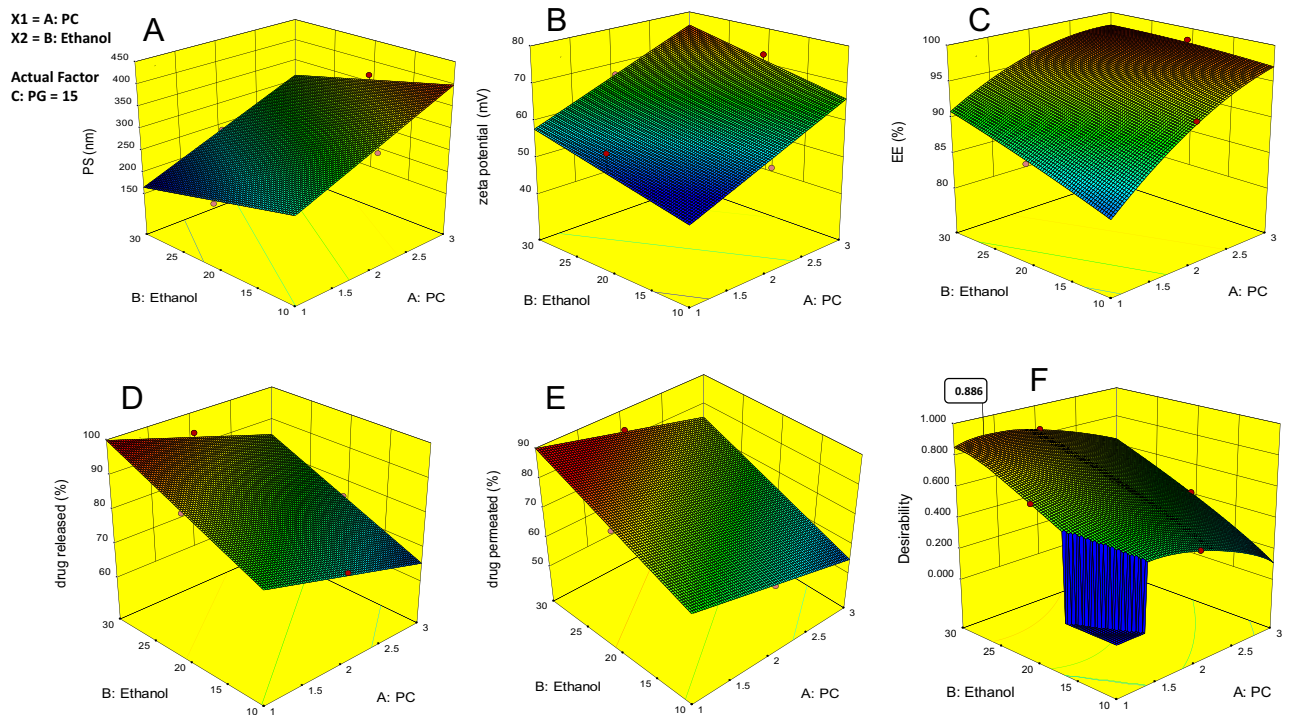


**Figure 1** Response surface plot for the effect of independent variables on (**A**) particle size, (**B**) ZP, (**C**) EE%, (**D**) % drug released over 24 hr, (**E**) % drug permeated over 24 hr and (**F**) desirability of the optimized ethosomal RP formula.

## Zeta Potential of Ethosomal RP Formulations

Zeta potential (ZP) refers to the total charges of the surface achieved by the particles, indicating the system's stability. ZP value of about ± 30 mV indicates a stable dispersion due to the force of repulsion of adjacent particles.[55,56] If the value of ZP is low, attraction overcomes repulsion, and the mixture forms likely coagulates.[57] In this study, ZP values of all ethosomal formulations ranged from −51 ±8.35 to −77.5 ±3.99 mV (Table 1), proving that the ethosomal vesicles have sufficient charges that prevent their aggregation. In this study, all of the prepared ethosomal formulations possess negative ZP values. The influence of the concentration of PC (A), concentration of ethanol (B), and concentration of PG (C) on the ZP of the ethosomes is graphically illustrated as 3-D surface plots in (Figure 1B). Among the three investigated independent variables, only the concentration of PC and ethanol significantly influenced the ZP (p= 0.0001). It was found that upon increasing the PG, ZP insignificantly decreased (p= 0.3598). The negative charge of the phospholipid may be due to phosphate group ionization. Accordingly, when the concentration of phospholipids increased, the negative charge of the vesicles increased.[58,59] Regarding the concentration of ethanol (B), ZP increased when the ethanol concentration increased.[60,61] Similar results have been reported previously, indicating that ethanol provides a net negative charge of the ethosomal surface, thus avoid vesicles aggregation due to repulsion between vesicles.[59]

## EE% of Ethosomal RP Formulations

Entrapment efficiency is one of the important parameters to evaluate the system's success to entrap the drug. Percent of RP entrapped ranged from 82.01±6.02 to 98.86±5.01% (Table 1). The effect of the concentration of PC (A), concentration of ethanol (B), and the concentration of PG (C) on the EE% of the ethosomes is graphically illustrated as 3-D surface plots in (Figure 1C). Increasing the concentration of PC (A), ethanol (B), and PG (C) were found to significantly influence the EE% (p = 0.0001) for A, B, and (p = 0.0223) for C. Results revealed that the concentration of PC significantly improved the EE%. It was found that raising the concentration of PC from 1% to 3% caused a simultaneous increase in EE%[62] of RP, which may be due to the lipophilic nature of RP. The EE % values of ethanol at concentration 30% contained ethosomes formulations were superior to those of ethanol at

concentration 10%, which might be succumbed to the co-solvent effect of ethanol which plays a significant role in enhancing the solubility of a lipophilic drug in the polar ethosome phase and allows additional amounts of drugs in ethosome's aqueous core.[50,63] Similarly, PG at concentration 15% based ethosomes formulations exhibited significantly higher EE% than those containing PG at concentration 5%, p <0.05. A possible explanation may be the ability of PG to increase the solubility of the drug in water-ethanol mixtures.[64,65]

## In-vitro Drug Release Studies

The release pattern of RP from ethosomes was investigated to verify if the ethosomal RP could release RP in a sustained manner. It was observed that the release manner was rapid from the free RP suspension, with about 56% of the RP being released in the first 3h (Figure S1A and B) (supplemental file). In contrast, the RP in ethosomes demonstrated a slow and controlled release, with about 26.29% to 48.54% (Figure S1A and B) (supplemental file). The in-vitro release study from ethosomal formulations of the RP being released within 24h ranged from 62.48±8.54 to 97.9±3.92% (Table 1). The % of RP released from the suspension is faster and higher than the RP released from the ethosomes; this may be due to the reservoir effect of the vesicular system, which delays RP release from the ethosome.[66] The effect of the concentration of PC (A), concentration of ethanol (B), and concentration of PG (C) on the % of RP released from the ethosomes is graphically illustrated as 3-D surface plots in Figure 1D. Concerning PC (A) concentration, ANOVA demonstrated that this variable significantly decreases % of RP released from the ethosomes (P=0.0001) with increasing its concentration. Contradictory to this, increasing the concentration of ethanol (B) and PG were found to improve the % of RP released from the ethosomes significantly (P <0.0001 and 0.0016, respectively). As the PC concentration increased, % of RP released from ethosomes reduced; this may be due to increased vesicle rigidity, which decreases the release of the drug from vesicles.[47,67] It was noticed that increasing the concentration of ethanol significantly increases the RP release rate; this indicates that it increases liquefaction and permeability of the drug, facilitating its diffusion through membranes and leading to an increase in the drug release.[65,68] Release data analysis revealed that almost all ethosomal RP formulations follow Higuchi's matrix model with the highest $R^2$ value, indicating slow and sustained RP release.[53]

## Ex-vivo Permeability Study

Ex-vivo skin permeation profiles of ethosomal RP via rat skin relative to RP suspension were represented in Figure S2A and B (supplemental file). The ethosomal formulations verified higher skin permeation than drug suspension containing an equal quantity of RP (p <0.05). From Figure S2 (supplemental file). It was noticed that 42.95% of RP suspension was permeated via rat skin over 24 h; meanwhile, the % of RP was permeated from ethosomes ranged from 51.53 ±4.33 to 85.18 ±5.61% (Table 1). The increased drug permeation of ethosomal RP compared to RP suspension is due to the flexibility of ethosomal vesicles and their ability to bypass the stratum corneum. Another reason is the presence of ethanol which has a fluidizing effect on membrane lipids that allows drug penetration via SC till dermal layers and increases the solubility of the hydrophobic drug (RP).[69–71] The effect of the concentration of PC (A), concentration of ethanol (B), and concentration of PG (C) on the % of RP permeated from the ethosomes is graphically illustrated as 3-D surface plots in (Figure 1E). Concerning PC (A) concentration, ANOVA showed that this variable significantly decreases the percentage of RP permeated from the ethosomes (P=0.0001). In contrast, increasing the concentrations of ethanol (B) and PG were found to improve the percentage of RP significantly permeated from the ethosomes (P <0.0001 and 0.0012, respectively). In our study, PC at concentration 1% contained ethosomes were more readily permeated than other ethosomes contained PC at a concentration of 3%. The observed variation might be claimed to increase vesicle rigidity.[65,67,72] Additionally, 30% of ethanol results in a significantly higher RP permeation than 10% ethanol. A possible explanation is that ethanol is a well-known permeation enhancer as it increases cell membrane lipid fluidity.[69] Furthermore, the combination of ethanol and PG enables the drug to more easily penetrate the skin.[46] The prepared ethosomal formulations showed superior permeation characteristics compared to RP suspension evidenced from shorter lag time, higher permeability coefficient with enhanced E.I. from 1.06 to 1.76 as revealed in (Table 4).

## Selection of the Optimal Formulation

According to the analyzed data, there was an insignificant lack of fit for any of the responses. Optimization was achieved using the desirability approach to obtain the levels of A, B, and C with maximization of $Y_3$, $Y_4$, and $Y_5$, and minimization of $Y_1$ according to the developed polynomial equations. The

**Table 4** Ex vivo Permeation Parameters of Ethosomal RP Formulations

| Formulation | Lag Time (min) | Jss (μg/cm$^2$ h) | Kp (cm/h) | EI |
|---|---|---|---|---|
| F1 | 25.4961 | 19.21 | 0.01921 | 1.24 |
| F2 | 39.60187 | 25.62 | 0.02562 | 1.66 |
| F3 | 25.13599 | 22.87 | 0.02287 | 1.48 |
| F4 | 56.02113 | 17.04 | 0.01704 | 1.1 |
| F5 | 15.37897 | 24.54 | 0.02454 | 1.59 |
| F6 | 16.5859 | 21.13 | 0.02113 | 1.37 |
| F7 | 35.55245 | 21.45 | 0.02145 | 1.39 |
| F8 | 55.94397 | 16.42 | 0.01642 | 1.06 |
| F9 | 25.40839 | 27.18 | 0.02718 | 1.76 |
| F10 | 52.13483 | 24.03 | 0.02403 | 1.56 |
| F11 | 62.58813 | 21.56 | 0.02156 | 1.4 |
| F12 | 44.97833 | 20.77 | 0.02077 | 1.34 |
| F13 | 36.67233 | 17.67 | 0.01767 | 1.14 |
| F14 | 22.37778 | 21.6 | 0.0216 | 1.4 |
| F15 | 51.42857 | 18.97 | 0.01897 | 1.23 |
| RP suspension | 73.12621 | 15.45 | 0.01545 | – |

formulation was chosen by the design expert® software and composed of 1.331% w/w of PC, 30% v/v of ethanol, and 15% v/v of PG was the optimum formulation whose overall desirability was 0.886 as the best formulation to achieve this goal, as illustrated in (Figure 1F). As depicted in (Table 5), the optimal formulation observed values were highly comparable to the predicted ones, showing a small percentage of prediction error fluctuated from 0.68% to 2.95% for different responses, confirming the adequacy and fitness of the suggested mathematical model for speculation of dependent responses. In total, this formulation was selected for further investigation. Also, the response surface of all measured parameters was well represented by the contour plot. The contour lines representing the effect of different formulating factors on different responses were demonstrated (Figure 2). Also, both zeta potential and particle size distribution curves are shown in Figure S6 and 7 (supplemental file).

## Morphology of Optimized Ethosomal RP Formulation

The optimized ethosomal formulation morphology was investigated using T.E.M. imaging (Figure 3). The formed vesicles were uniform and spherical in shape with a smooth surface and without any noted aggregation. Morphological investigation confirms the particle size values determined with DLS.

## Physical Stability of the Optimized Ethosomal RP Formulation

The stability, based on particle size, ZP, and EE% of the optimized ethosomal RP formulation after 3 months of storage at 4°C and 25°C, was evaluated. There were insignificant changes in particle size (increased from 195.8 ±5.45 to 206.5±8.15 nm at 4°C and to 217.1±3.25 nm at 25°C), Zeta potential (decreased from −62.1±2.85 to −54.2 ±2.65 mV at 4°C and to −51.3±2.34 mV at 25 °C) and EE% (decreased from 92.63±4.33 to 85.77±5.23% at 4°C and to 81.28±4.35% at 25°C) after 90 days as shown in (Figure 4). Vesicle rigidity may cause the excellent stability of the optimized ethosomal RP formulation[68] and high ZP, which prevents vesicle aggregation.[73,74]

## Experimental Design and Data Analysis of Hydrogel Formulations

Historical Data Design effectively assesses the variables that will probably impact the properties of a new drug delivery system. It can concurrently analyze the impact of multivariables on the characteristics of the drug delivery system. It was used to design eight gel formulations, which were statistically analyzed using Design-Expert® software. The experimental run and the measured parameters are listed and computed (Table 2).

**Table 5** Predicted and Experimental Values of the Optimal Ethosomal RP Formulations

| Solution | PC Conc. | Ethanol Conc. | PG Conc. | $Y_1$ | $Y_2$ | $Y_3$ | $Y_4$ | $Y_5$ | Desirability |
|---|---|---|---|---|---|---|---|---|---|
| Predicted | 1.33 | 30 | 15 | 190.01 | 60.99 | 93.26 | 97.48 | 87.54 | 0.886 |
| Experimental | 1.33 | 30 | 15 | 195.80 | 62.10 | 92.63 | 96.63 | 85.98 | 0.886 |
| Bais % | – | – | – | 2.95 | 1.78 | 0.68 | 0.87 | 1.81 | – |

**Note**: Bias % = [(predicted value-experimental value)/experimental value]×100.

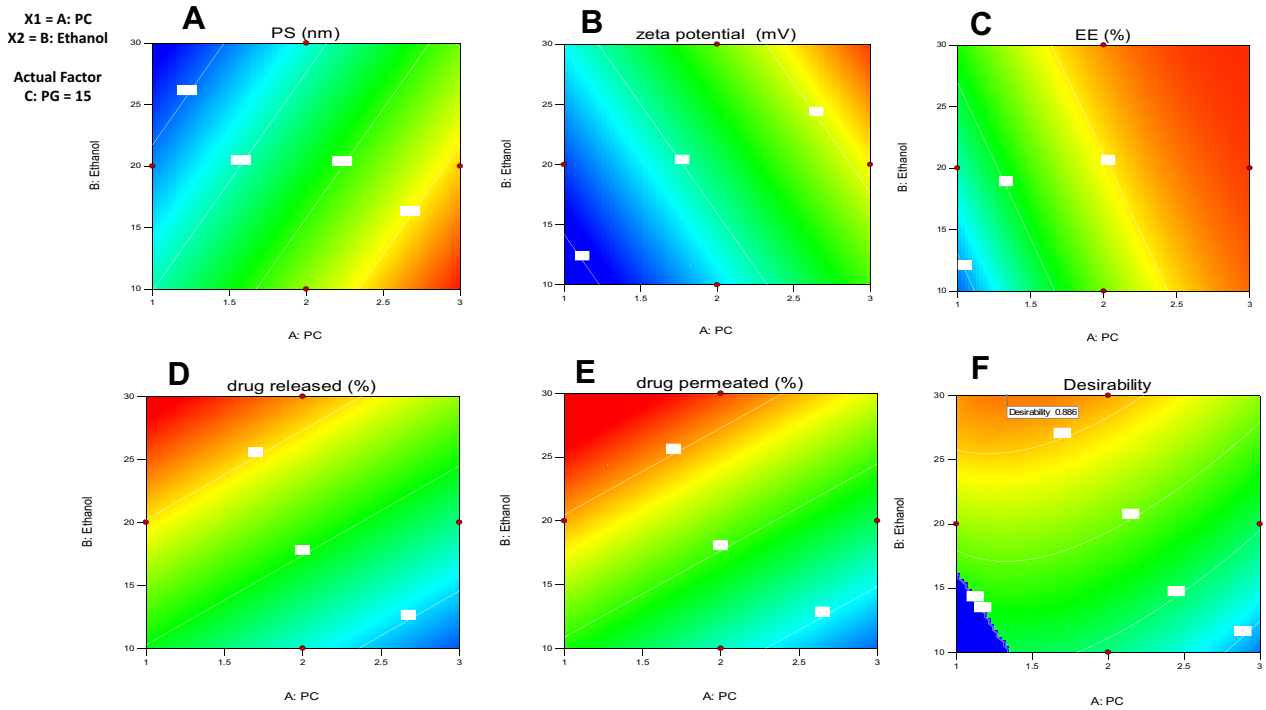


**Figure 2** Contour plot for the effect of independent variables on (**A**) particle size, (**B**) ZP, (**C**) EE%, (**D**) % drug released over 24 hr, (**E**) % drug permeated over 24 hr and (**F**) desirability of the optimized ethosomal RP formula.

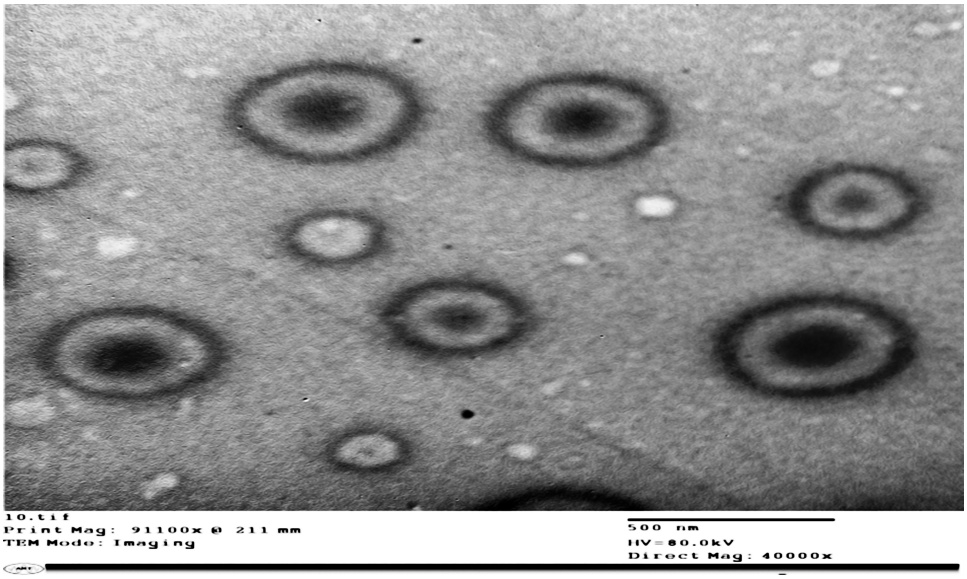


**Figure 3** Transmission electron micrograph of the optimized ethosomal RP formulation.

## Rheological Study

The viscosity of all hydrogel formulations ranges from 1272.32 to 6405.12 cP. It was observed that increasing polymer concentration from 1 to 2 causes the viscosity to increase. Viscosities of carbopol-based hydrogels are higher than those based on chitosan. High carbopol viscosity forms a colloidal dispersion that converts into a salt upon neutralization with triethanolamine, which in turn absorbs water and forms the crosslinks between polymer chains forming a stronger bond of

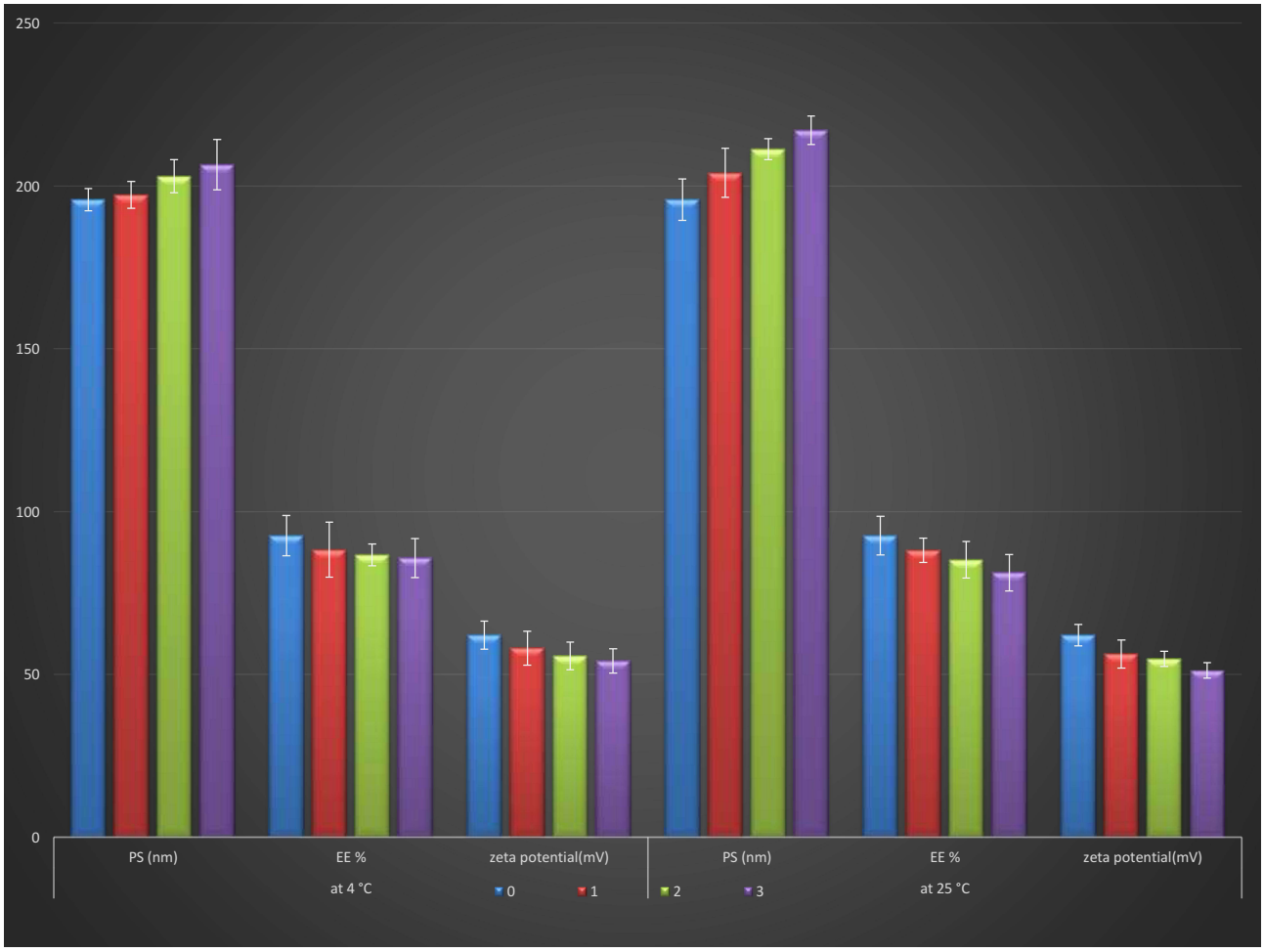


**Figure 4** Effect of storage at 4°C and 25°C for 3 months on particle size, ZP and EE % of the optimized Ethosomal RP formula.

microgel network.[75] It was observed that increasing DMSO concentration from 1 to 2 causes a decrease in viscosity; similar results were obtained using DMSO with carbopol hydrogel.[76,77] All hydrogel formulations exhibited shear rate thinning behavior with thixotropy (Figure 5). The results of the viscosity measurements for all hydrogel formulations at different values of shear rate are plotted in (Figure 6). Thixotropy, which is a desirable character in pharmaceutical gels, indicates decreasing the viscosity of the gel with increasing shear stress.

Moreover, after removing the shear stress, the viscosity slowly returns to the former state. Using the trapezoidal rule, the hysteresis loop area formed between the up and down curves of the rheograms was determined to indicate the degree of thixotropy. Farrow's constant ranges from 1.5 to 5.281 which confirmed pseudoplastic properties of the ethosomal hydrogel (Table 2).

## In-vitro Drug Release Study of Ethosomal Hydrogels

The release profiles of RP from the fabricated ethosomal hydrogels are graphically illustrated in Figure S3 (supplemental file). The % RP release from drug suspension within 24 h was approximately 98.21± 2.01%. The % of drug released from ethosomal gel after 24 h ranged from 53.54 ±4.81 to 89.39 ±3.84% as denoted in (Table 2). The explored model was statistically significant concerning residual analysis and ANOVA with an adequacy/precision ratio of 32.55, elucidating adequate signal. The quantitative effect of independent variables on the release of RP ethosomal gel coded values is represented by Equation (5).

$$Y_1 = 79.67 - 10.28\times_1 - 10.21X_2 + 4.38\ X_3 \quad (5)$$

The investigated independent variables showed a significant effect on the % drug release of various ethosomal gel ($p < 0.05$) (Figure 7A). With respect to polymer type, it was

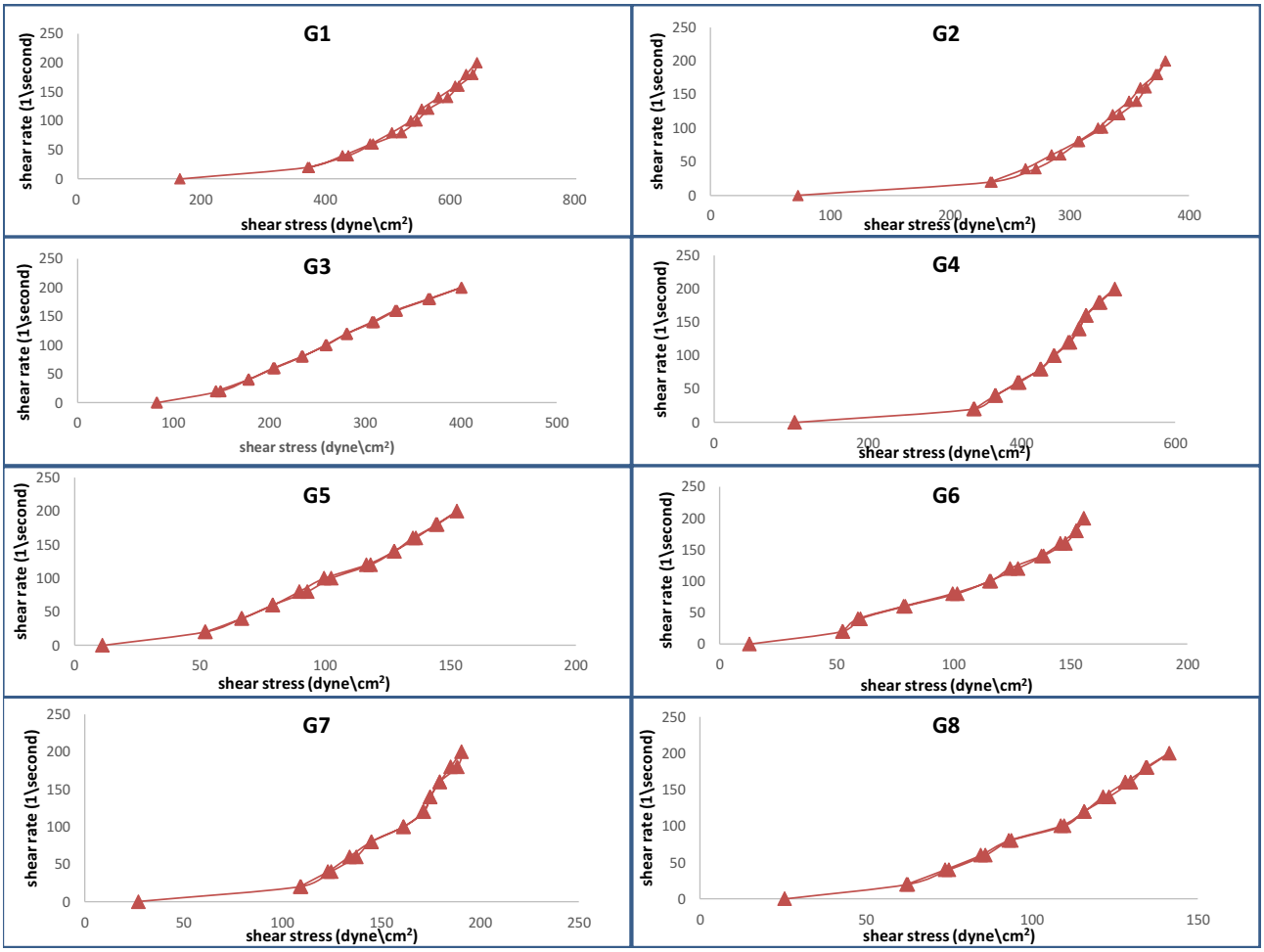


**Figure 5** Rheograms of RP hydrogel formulations; G1-G8.

observed that the % drug release values of carbopol-based hydrogels were significantly higher than that of chitosan polymer ($p < 0.05$). As has already been determined, rapid release of carbopol could be due to repulsion between the negatively charged RP ethosomes and the negative nucleus of Carbopol 971P and attraction between the negatively charged RP ethosomes and the cationic chitosan hydrogel matrix.[78] A notable finding is that % drug release was decreased significantly with increasing polymer concentration ($p= 0.0007$); this may be due to increased viscosity of gel which interrupts the release of the drug from the gel matrix. Also, % drug release was significantly increased with increasing surfactant concentration ($p= 0.0154$), which acts as a permeation enhancer as it increases the fluidity of stratum corneum lipids.[79–81]

## Ex-vivo Permeability Study of RP Ethosomal Hydrogel

Ex-vivo skin permeation profiles of RP ethosomal hydrogel through rat skin were represented in Figure S4 (supplemental file). The investigated ethosomal hydrogel showed ex-vivo permeation in the range of 38.25±3.62 to 75.47 ±3.55% (Table 2) versus 24.59±3.05% for the RP suspension. ANOVA statistical analysis revealed that the sequential model recommended for estimating the % drug permeation response was a linear model with an adjusted $R^2$ value of 0.9732, suggesting that the model could clarify nearly 97% of the entire variations in the transdermal permeation. Thus, the % drug permeation could be correlated to the three factors using the following equation in terms of coded value:

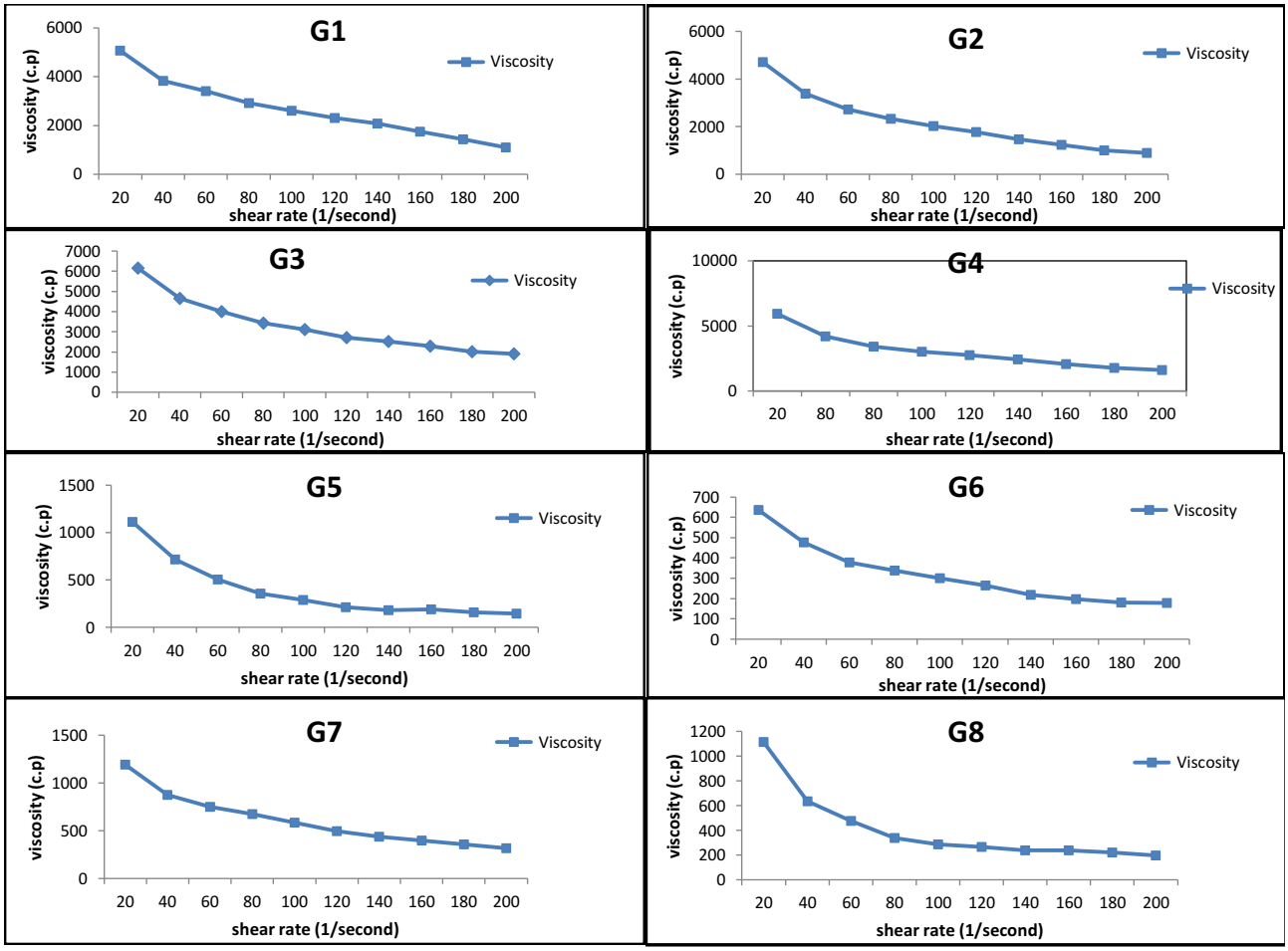


**Figure 6** Flow curves of RP hydrogel formulations; G1-G8.

$$Y_2 = 62.06 - 12.61X_1 - 9.2X_2 + 4.92X_3 \qquad (6)$$

The effect of the formulation variables on the % drug permeation of RP ethosomal hydrogel is illustrated in (Figure 7B). ANOVA indicated a significant effect of all $X_1$, $X_2$, and $X_3$ on drug permeation (p= 0.0001, 0.006, and 0.0465, respectively). It was observed that the highest diffusion of RP from its hydrogel formulations was obtained in the Carbopol 971P hydrogel matrix. A plausible explanation for these results is that the anionic polymer Carbopol 971P is reported to demonstrate permeation enhancing properties as it can bind $Ca^{+2}$ present in the epithelium tissue.[82] Secondly, the polymer chain of Carbopol 971P undergoes decoiling due to electrostatic repulsion between its ionized carboxyl groups. Thus, swelling of Carbopol 971P occurs due to the absorption of water from the epithelial tissue, which causes intimate penetration into the skin and hence localizes the formulation in the skin and enhancing the drug concentration gradient across the epithelium;[83] this results in high dissolution and diffusion of the drug from the hydrogels due to extensive swelling of the ionized Carbopol 971P.[84] Increasing polymer concentration causes a decrease % of drug permeated. On the contrary, with increasing DMSO concentration, which increase % drug permeated due to reasons discussed before in hydrogel release study.

## Selection of the Optimized RP Ethosomal Hydrogel

Design Expert® software was used to optimize the prepared eight formulations based on the Historical Data Design. The optimum formulation (achieving the highest values of % drug release and % drug permeation) was composed of carbopol 1% and 2% of DMSO. This formulation showed a % drug release of 88.5±5.82% and % drug permeation of 75.32±3.88%. The desirability

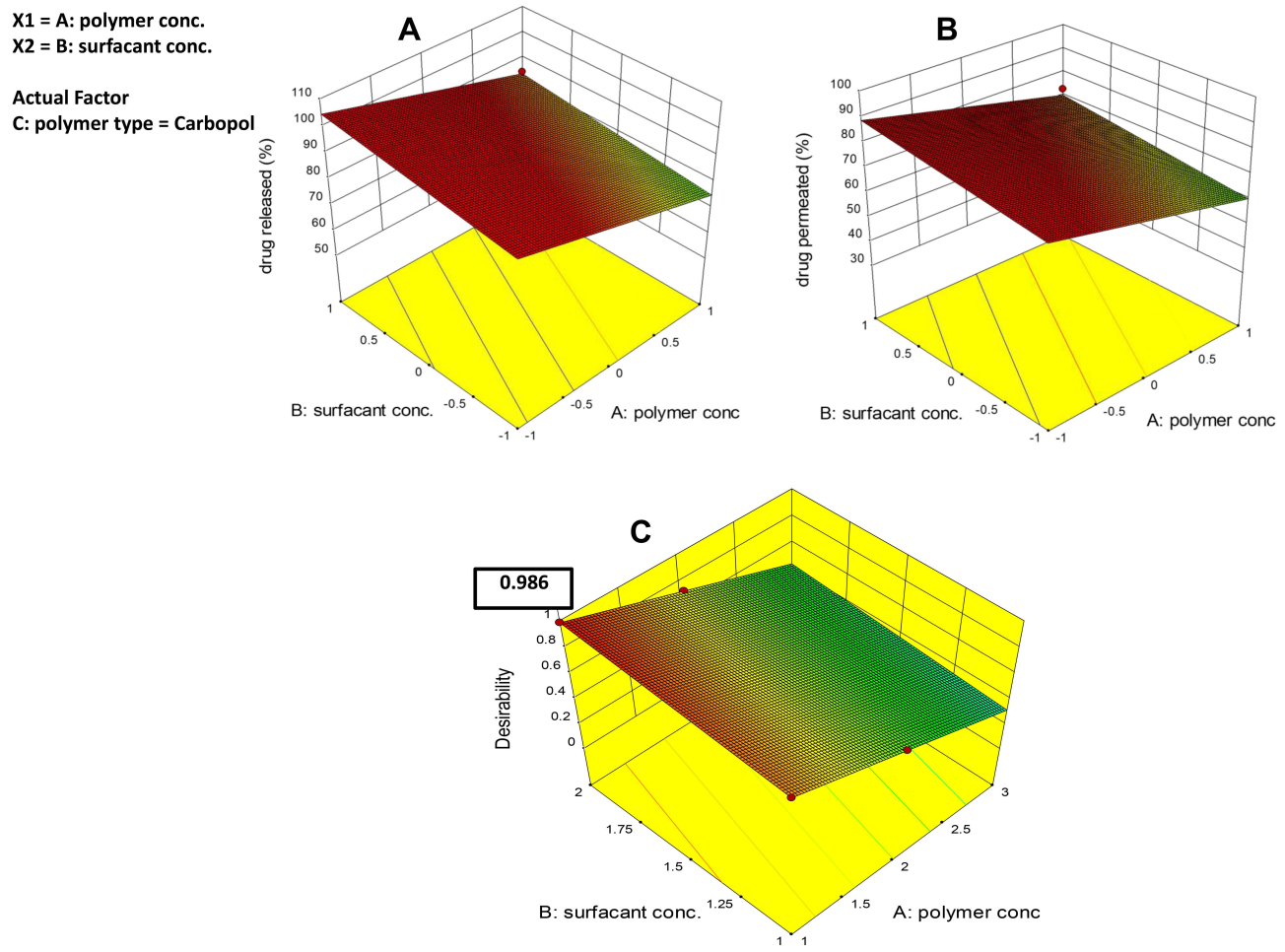


**Figure 7** Response surface plot for the effect of independent variables on (**A**) % drug released over 24 h, (**B**) % drug permeated over 24 h, (**C**) desirability of the optimized RP ethosomal hydrogel.

constraints for the optimized were investigated with an overall desirability value of 0.986, as illustrated in Figure 7C.

## Characterization of Optimized RP Ethosomal Hydrogel

### In-vitro Drug Released

The % of RP released from optimized RP ethosomal hydrogel and control gel was displayed in Figure S5 (supplementary file). About 94.54±4.73% of RP was released from control gel compared to 88.75±4.64% of RP released from optimized RP ethosomal hydrogel within 24h; this may be due to the retardation of drug release from ethosome. The optimized hydrogel drug release follows Higuchi's matrix model with $R^2$ of 0.913, indicating sustained drug release.

### Ex-vivo Drug Permeation

The % of RP permeated from optimized ethosomal hydrogel and control gel was displayed (Figure 8). The % of RP permeated from optimized RP ethosomal hydrogel and control gel were 79.47±2.34% and 22.64±3.54%. Meanwhile, the higher % of drug permeated from RP ethosomal hydrogel may be due to ethanol's presence, increasing drug solubility and leading to fluidization of membrane lipids, increasing their ability to permeate via skin layers.[71]

### Skin Irritation Studies

The control group (Figure 9A) shows more or less normal epidermal and dermal layers. Meanwhile, the tretinoin-treated group (Figure 9B) shows an area of excoriation with the accumulation of serum in the keratinous layer (scale crust) (black arrow), dilated congested blood vessels

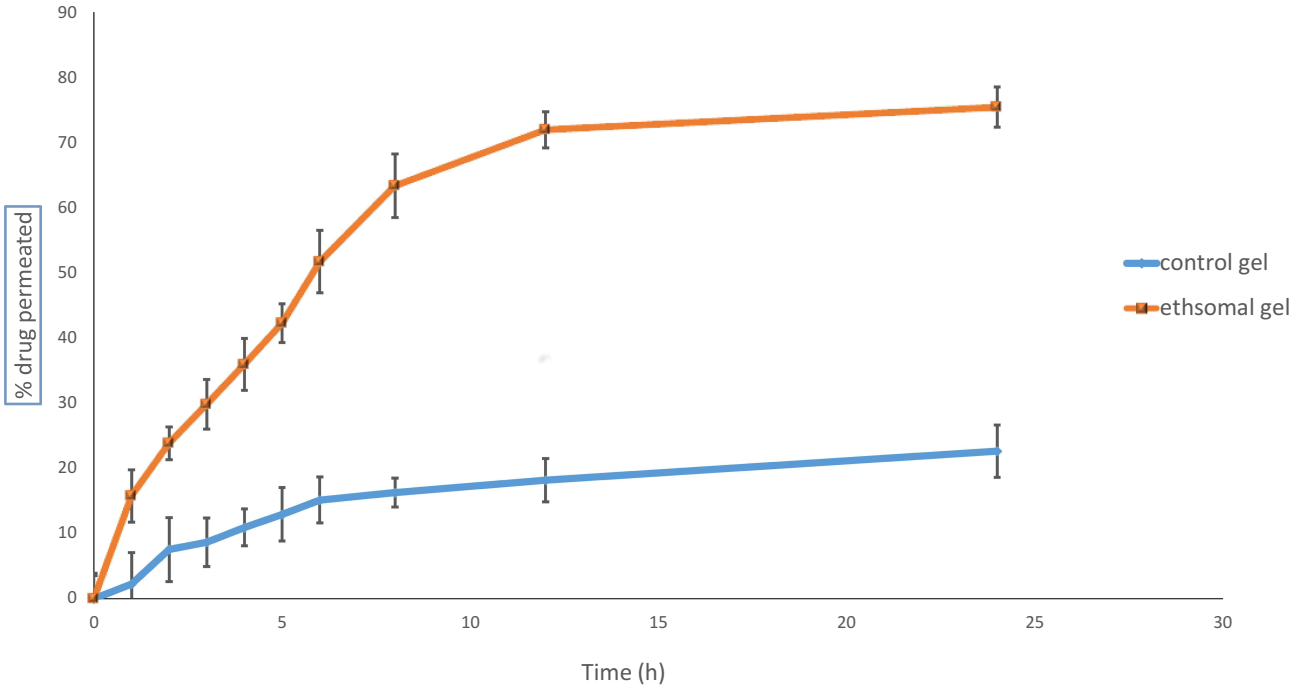


**Figure 8** % Drug permeated from control gel and optimized RP ethosomal hydrogel.

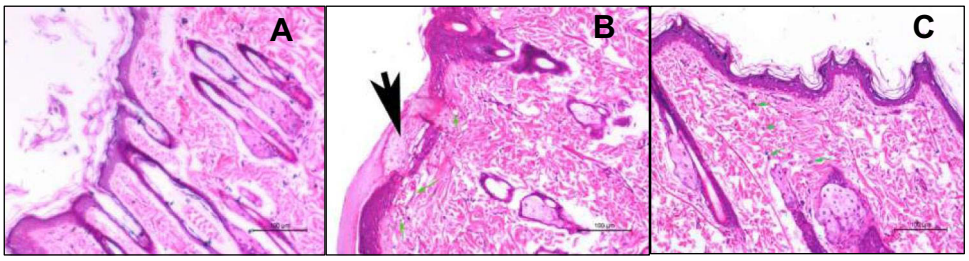


**Figure 9** Light photomicrographs showing histopathological sections of (**A**) rat skin of the control group, (**B**) rat skin of tretinoin cream treated group, and (**C**) rat skin of ethosomal RP hydrogel treated group. (H&E stain; Bar= 100μm).

in the superficial dermis (green arrows) which indicate the irritation of the epidermal layer.

The Retinyl palmitate-treated group (Figure 9C) shows an unremarkable epidermis, no congested dermal vessels. Only scattered eosinophils in the dermis are seen. Congestion was minimal compared to the tretinoin treated group, suggesting a lower reaction to the drug than the tretinoin.

## Clinical Evaluation of RP Ethosomal Hydrogel

The purpose of this prospective, split-face comparative clinical study was to compare the efficacy and tolerability of RP ethosomal hydrogel to topical tretinoin cream, which is known to be beneficial in treating mild to moderate facial acne vulgaris.[15] A total of 20 patients with facial acne vulgaris, 18 females and 2 males, with a mean age of 22.55±3.87 years, were included. There was no significant difference between the two sides of the face regarding the baseline number of total, non-inflammatory, and inflammatory acne lesions. In the present study, the therapeutic effect of the topical application of ethosomal RP hydrogel on mild to moderate acne vulgaris has been demonstrated for the first time. Both the marketed tretinoin and the ethosomal RP formulations demonstrated steady improvement of acne during treatment over the 6 weeks of the study.

### Evaluation of Lesion Count

Both sides of the face demonstrated a gradual decrease in acne lesion count with a significant reduction in total,

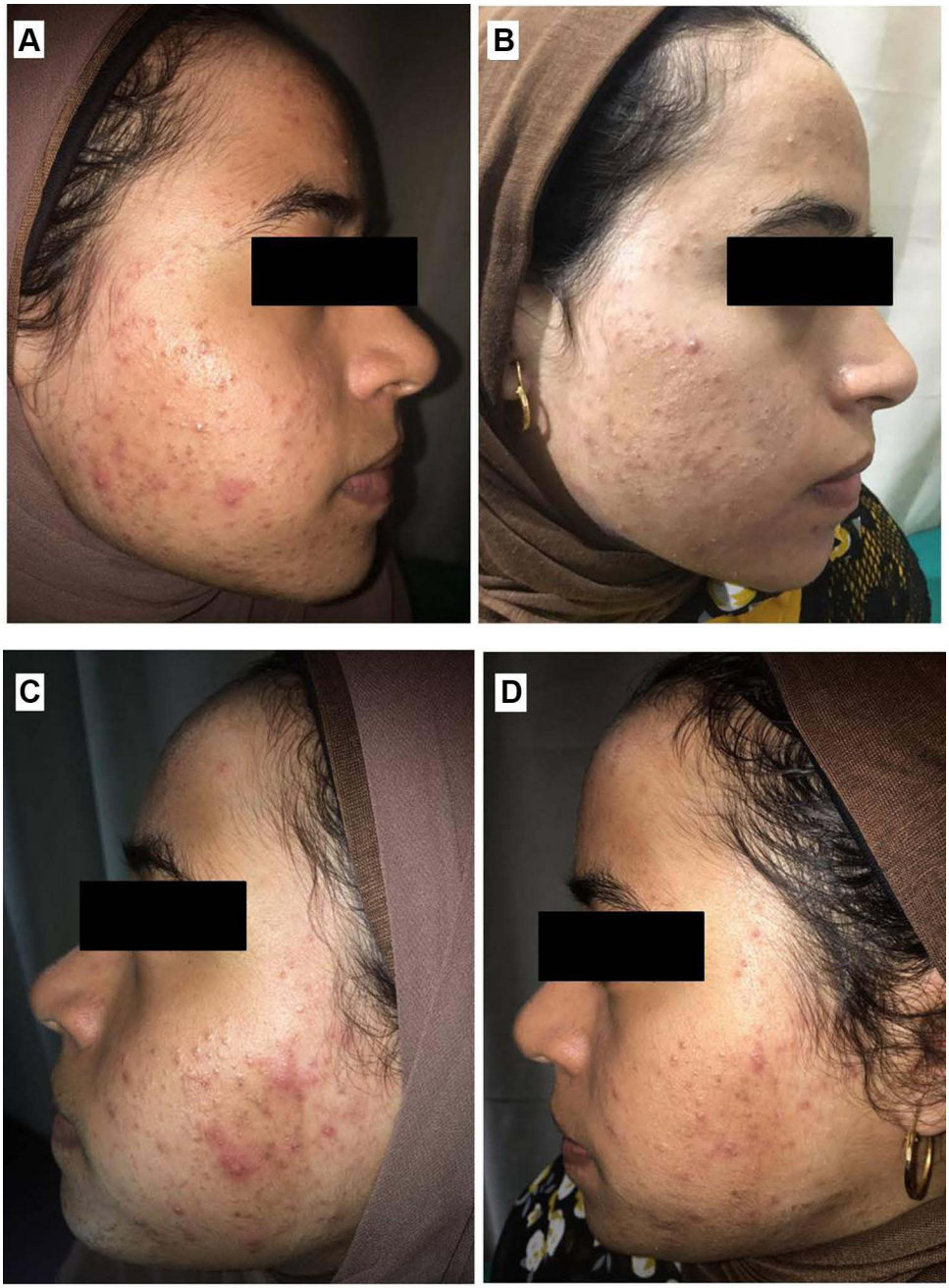


**Figure 10** Right side of face before (**A**) and after topical tretinoin (**B**). Left side of the face before (**C**) and after ethosomal RP hydrogel (**D**). Peeling and dryness noted after topical tretinoin.

inflammatory, and non-inflammatory lesion counts from baseline at 2, 4, and 6 weeks of treatment (Table 6).

Regarding the total lesion count, there was a significant decrease in both tretinoin and RP ethosomal hydrogel treated sides at week 6 compared to baseline (P<0.001 for both). There was also a significantly lower total lesion count on the RP ethosomal hydrogel treated side than on the tretinoin treated side (P=0.016) at week 6.

The mean non-inflammatory lesion number was significantly lower on the RP ethosomal hydrogel formulation treated side than on the tretinoin treated side (P=0.008) at week 6. Although both sides showed a significant reduction in the inflammatory lesion count at week 6 when compared to baseline (P=0.001 for both), there was no significant difference between the two sides (P=0.083). Some clinical studies have consistently demonstrated significant reductions in both non-inflammatory and

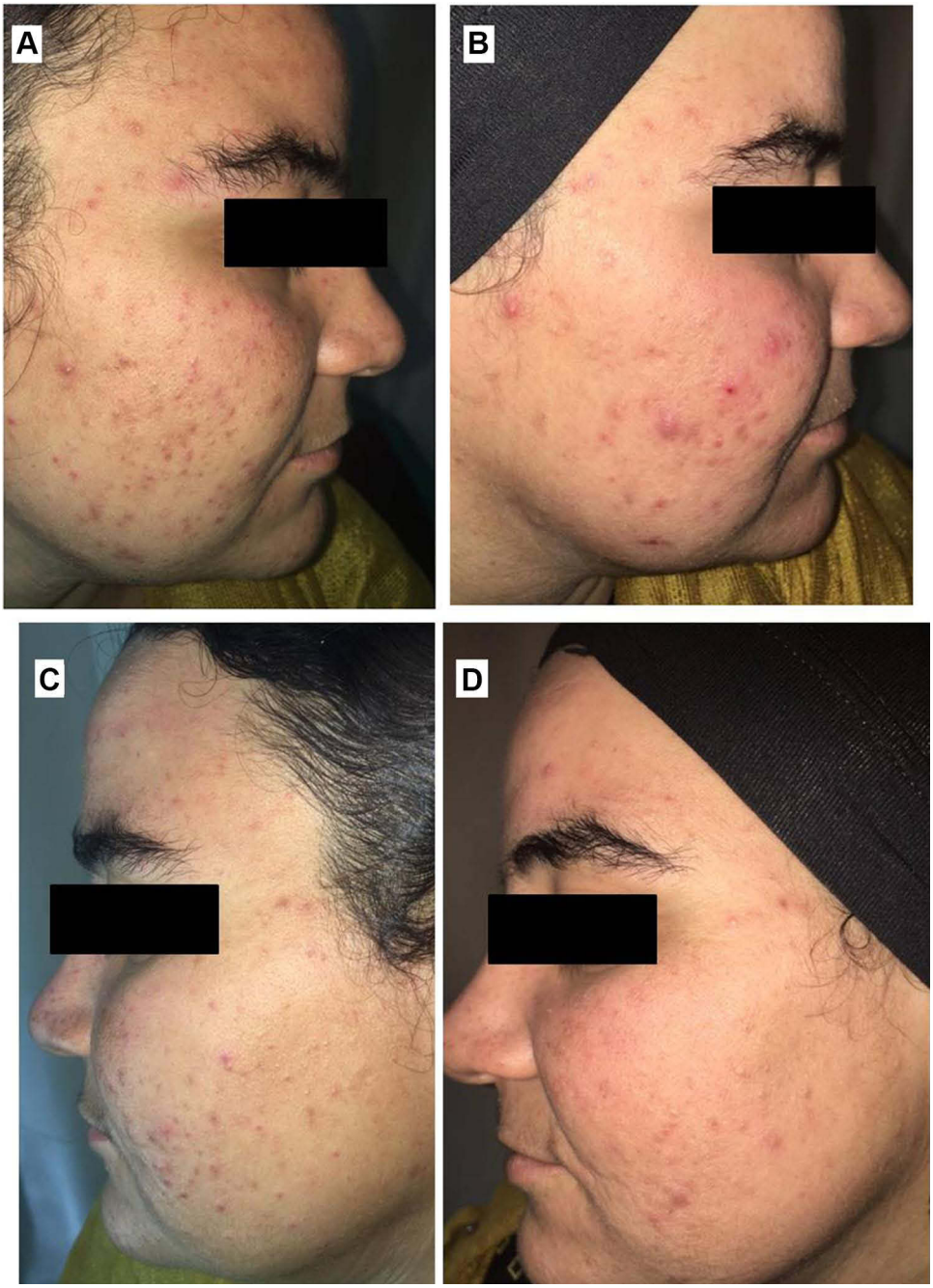


**Figure 11** Right side of face before (**A**) and after topical tretinoin (**B**). Left side of the face before (**C**) and after ethosomal RP hydrogel (**D**). Moderate erythema noted after topical tretinoin.

inflammatory acne lesions with topical tretinoin nano-delivery systems compared to the conventional topical formulations.[32,85,86]

RP ethosomal hydrogel-treated side showed a relatively greater mean percent reduction from baseline to week 6 in total, non-inflammatory and inflammatory lesion counts compared to tretinoin treated side (46.69% non-inflammatory lesions, 39.32% inflammatory lesions, and 39.95% total lesions vs 34.32%, 28.35%, and 28.49%, respectively). However, the difference was not statistically significant (P=0.071, P=0.432 and P=0.179, respectively); this may be due to the small size of the study sample and short treatment period. However, the clinical improvement of acne lesions was in favor of the RP ethosomal hydrogel treated side, which was clearly noticed by improvement in lesion size and visibility.

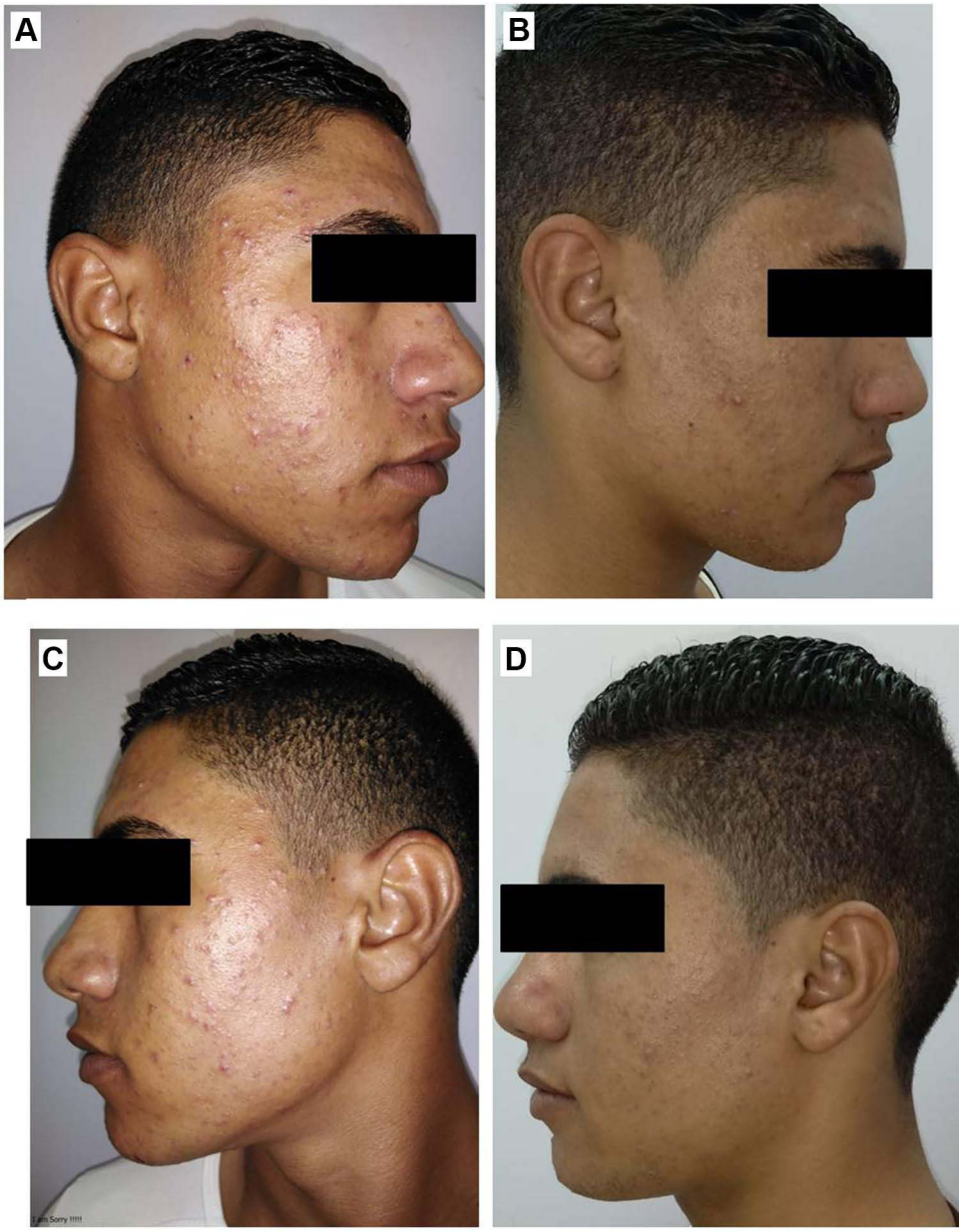


**Figure 12** Right side of face before (**A**) and after topical tretinoin (**B**). Left side of the face before (**C**) and after ethosomal RP hydrogel (**D**).

Several targeted topical retinoid delivery systems containing tretinoin, including microsphere and micronized formulation, were developed to improve efficacy and minimize tretinoin-associated cutaneous irritancy.[87,88] While the tretinoin microsphere gel effectively reduced non-inflammatory and inflammatory acne lesions, the incidence of skin-related adverse effects was still high.[89]

The development of a targeted topical delivery system is greatly required to improve or maintain efficacy and reduce this high incidence of adverse effects.

## Skin Tolerability

RP ethosomal hydrogel treatment was better tolerated compared to the marketed topical tretinoin. Local treatment-related skin reactions, including erythema, peeling, burning, and pruritus, were more frequent and more severe on the right side treated with conventional topical tretinoin. Almost all patients had no, or slight skin irritation on the ethosomal RP treated side (Table 7). Conventional topical retinoid formulations have proven to be effective in reducing acne vulgaris lesions.

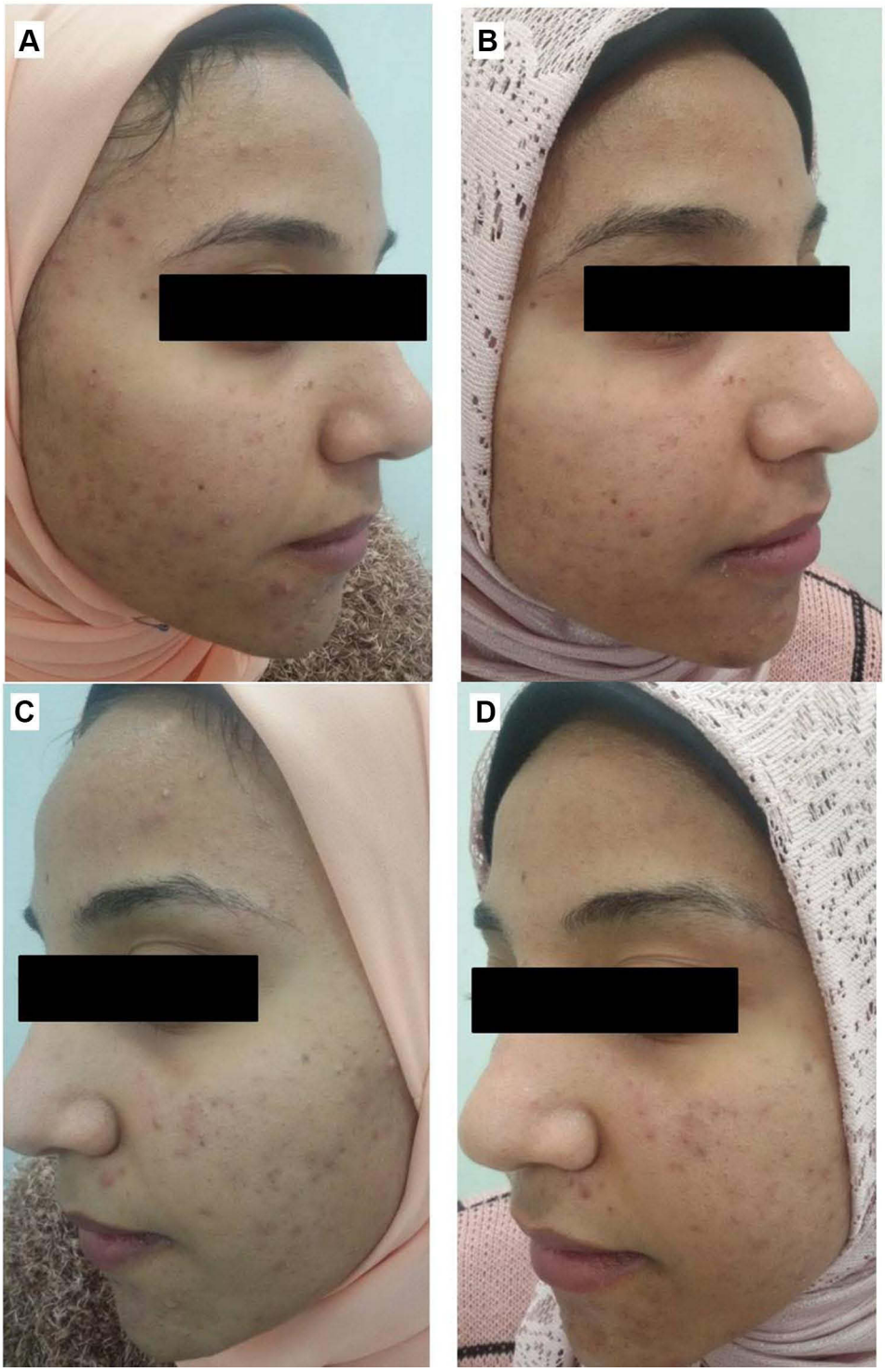


**Figure 13** Right side of face before (**A**) and after topical tretinoin (**B**). Left side of the face before (**C**) and after ethosomal RP hydrogel (**D**).

However, they are often poorly tolerated due to their potential for local skin irritation. The extremely low irritation potential is an outstanding advantage of the novel RP ethosomal hydrogel formulation; this demonstrates how the targeted topical retinoid delivery system enhances the clinical outcome of acne and overcomes the problems of local cutaneous irritation. Similar results were described using topical tretinoin-loaded proniosomes.[32] An additional factor for the improved skin tolerability observed for the topical treatment with

**Table 6** Mean Acne Lesion Count Before and After Treatment

| Lesion Count | Right Side (Conventional Tretinoin) | | Left Side (Ethosomal RP Hydrogel) | | P-value[b] |
|---|---|---|---|---|---|
| | Mean ± SD | P-value[a] | Mean ± SD | P-value[a] | |
| **Non-inflammatory lesions** | | | | | |
| Baseline | 9.80 ± 5.27 | | 9.35 ± 4.99 | | 0.529 |
| After 2 weeks | 7.79 ± 4.93 | 0.016 | 6.37 ± 3.39 | 0.002 | |
| After 4 weeks | 6.35 ± 3.51 | < 0.001 | 4.70 ± 2.342 | 0.001 | |
| After 6 weeks | 6.45 ± 3.75 | < 0.001 | 4.65 ± 2.56 | < 0.001 | 0.008 |
| Final % reduction | 34.32 ± 0.2 | | 46.69 ± 0.24 | | 0.071 |
| **Inflammatory lesions** | | | | | |
| Baseline | 9.3 ± 6.47 | | 9.2 ± 5.88 | | 0.706 |
| After 2 weeks | 7.42 ± 4.86 | 0.006 | 6.11 ± 3.59 | 0.007 | |
| After 4 weeks | 6 ± 4.32 | 0.005 | 4.55 ± 3 | 0.001 | |
| After 6 weeks | 6.2 ± 4.1 | 0.001 | 4.6 ± 2.81 | 0.001 | 0.083 |
| Final % reduction | 28.35 ± 0.32 | | 39.32 ± 0.37 | | 0.432 |
| **Total lesions** | | | | | |
| Baseline | 19.1 ± 8.39 | | 18.55 ± 8.42 | | 0.587 |
| After 2 weeks | 15.21 ± 6.96 | 0.005 | 12.47± 4.91 | 0.004 | |
| After 4 weeks | 12.35 ± 5.57 | < 0.001 | 9.25 ± 3.99 | 0.001 | |
| After 6 weeks | 12.65 ± 5.62 | < 0.001 | 9.25 ±3.89 | < 0.001 | 0.016 |
| Final % reduction | 28.49 ± 0.21 | | 39.95 ± 0.24 | | 0.179 |

**Notes**: [a]Comparison vs baseline within the same treatment side. [b]Comparison of the two treated sides. Significance is considered at $p < 0.05$.

RP ethosomal hydrogel in the current study could be retinoid use in an ester form (i.e. retinyl palmitate), thereby avoiding the carboxyl end group, which is responsible for the adverse skin effects. Clinical photographs that illustrate the improvement of acne lesions on both treatment sides are shown in Figures 10–13.

Finally, in this clinical study, both the marketed tretinoin and RP ethosomal hydrogel demonstrated steady improvement of acne during treatment over the 6 weeks of the study. While the results for inflammatory acne lesions were comparable between the two treatments, RP ethosomal hydrogel was superior to marketed tretinoin in reducing non-inflammatory comedonal lesions, suggesting its prominent comedolytic effect. Moreover, the extremely low irritation potential of this novel formulation was clearly demonstrated.

## Conclusion

RP was successfully encapsulated into ethosomes by ethanol injection technique for the topical treatment of acne. Box–Behnken design was used to optimize the ethosomes. The optimized ethosomal RP formulation contained 1.331% (w/w) of PC, 30% (w/w) of ethanol, and 15% (w/w) of PG showed small particle size with spherical morphology and high RP. EE%. The ex-vivo permeation studies showed that the loading of RP into ethosomes had enhanced the permeation of the drug through rat skin. Then, the optimized RP ethosome formulation was then incorporated into a hydrogel for clinical investigation. In a split-face clinical study, RP ethosomal hydrogel showed comparable efficacy to conventional tretinoin formulation, with a remarkable effect over the marketed tretinoin formulation in reducing non-inflammatory acne lesions. Moreover, it was found to have excellent tolerability with no or minimal local treatment-related skin reactions such as erythema, peeling, burning, and pruritus in treated volunteers compared to the conventional cream.

Therefore, RP-loaded ethosomal formulation constitutes a novel approach for the topical therapy of acne and represents an attractive alternative to minimize skin irritation induced by conventional marketed tretinoin formulation.

**Table 7** Local Adverse Effects in the Two Treatment Sides

| Side Effect | Right Side (Conventional Tretinoin) | Left Side (Ethosomal RP) | p-value |
|---|---|---|---|
| **Erythema, n (%)** | | | |
| No | 0 (0) | 7 (35) | < 0.001 |
| Mild | 3 (15) | 12 (60) | |
| Moderate | 15 (75) | 1 (5) | |
| Severe | 2 (10) | 0 (0) | |
| **Peeling, n (%)** | | | |
| No | 0 (0) | 7 (35) | < 0.001 |
| Mild | 7 (35) | 12 (60) | |
| Moderate | 11 (55) | 1 (5) | |
| Severe | 2 (10) | 0 (0) | |
| **Burning, n (%)** | | | |
| No | 0 (0) | 3 (15) | < 0.001 |
| Mild | 5 (25) | 15 (75) | |
| Moderate | 11 (55) | 2 (10) | |
| Severe | 4 (20) | 0 (0) | |
| **Pruritus, n (%)** | | | |
| No | 1 (5) | 4 (20) | < 0.001 |
| Mild | 1 (5) | 15 (75) | |
| Moderate | 12 (60) | 1 (5) | |
| Severe | 6 (30) | 0 (0) | |

## Acknowledgments

We express our gratitude to Dr. Ahmed Shawky, Department of Dermatology, Venereology and Andrology, Faculty of Medicine, Assiut University, as well as Hebatullah Abd Elrahem Fargly, Department of Medical-Surgical Nursing, Faculty of Nursing, Assiut University to complete this work.

## Disclosure

The authors report no conflicts of interest in this work.

## References

1. Dréno B. What is new in the pathophysiology of acne, an overview. *J Eur Acad Dermatol Venereol*. 2017;31:8–12. doi:10.1111/jdv.14374
2. Chan H, Chan G, Santos J, Dee K, Co JK. A randomized, double-blind, placebo-controlled trial to determine the efficacy and safety of lactoferrin with vitamin E and zinc as an oral therapy for mild to moderate acne vulgaris. *Int J Dermatol*. 2017;56(6):686–690. doi:10.1111/ijd.13607
3. Garofalo V, Cannizzaro MV, Mazzilli S, Bianchi L, Campione E. Clinical evidence on the efficacy and tolerability of a topical medical device containing benzoylperoxide 4%, retinol 0.5%, mandelic acid 1% and lactobionic acid 1% in the treatment of mild facial acne: an Open Label Pilot Study. *Clin Cosmet Investig Dermatol*. 2019;12:363. doi:10.2147/CCID.S182317
4. Fox L, Csongradi C, Aucamp M, Du Plessis J, Gerber M. Treatment modalities for acne. *Molecules*. 2016;21(8):1063. doi:10.3390/molecules21081063
5. Nast A, Rosumeck S, Erdmann R, Alsharif U, Dressler C, Werner R. Methods report on the development of the European evidence-based (S3) guideline for the treatment of acne–update 2016. *J Eur Acad Dermatol Venereol*. 2016;30(8):e1–e28. doi:10.1111/jdv.13783
6. Thiboutot DM, Dréno B, Abanmi A, et al. Practical management of acne for clinicians: an international consensus from the global alliance to improve outcomes in acne. *J Am Acad Dermatol*. 2018;78(2):S1–S23.e21. doi:10.1016/j.jaad.2017.09.078
7. Zaenglein AL, Pathy AL, Schlosser BJ, et al. Guidelines of care for the management of acne vulgaris. *J Am Acad Dermatol*. 2016;74(5):945–973. e933.
8. Gollnick H. From new findings in acne pathogenesis to new approaches in treatment. *J Eur Acad Dermatol Venereol*. 2015;29:1–7.
9. Antoniou C, Kosmadaki MG, Stratigos AJ, Katsambas AD. Photoaging. *Am J Clin Dermatol*. 2010;11(2):95–102. doi:10.2165/11530210-000000000-00000
10. Shamma RN, Sayed S, Sabry NA, El-Samanoudy SI. Enhanced skin targeting of retinoic acid spanlastics: in vitro characterization and clinical evaluation in acne patients. *J Liposome Res*. 2019;30(1):1–8. doi:10.1080/08982104.2019.1577256
11. Raza K, Singh B, Singla S, et al. Nanocolloidal carriers of isotretinoin: antimicrobial activity against Propionibacterium acnes and dermatokinetic modeling. *Mol Pharm*. 2013;10(5):1958–1963. doi:10.1021/mp300722f
12. Ridolfi DM, Marcato PD, Justo GZ, Cordi L, Machado D, Durán N. Chitosan-solid lipid nanoparticles as carriers for topical delivery of tretinoin. *Colloids Surf B Biointerfaces*. 2012;93:36–40. doi:10.1016/j.colsurfb.2011.11.051
13. Thielitz A, Gollnick H. Topical retinoids in acne vulgaris. *Am J Clin Dermatol*. 2008;9(6):369–381. doi:10.2165/0128071-200809060-00003
14. Silva EL, Carneiro G, de Araújo LA, et al. Solid lipid nanoparticles loaded with retinoic acid and lauric acid as an alternative for topical treatment of acne vulgaris. *J Nanosci Nanotechnol*. 2015;15(1):792–799. doi:10.1166/jnn.2015.9184
15. Kolli SS, Pecone D, Pona A, Cline A, Feldman SR. Topical retinoids in acne vulgaris: a systematic review. *Am J Clin Dermatol*. 2019;20(1):1–21. doi:10.1007/s40257-018-0398-x
16. Kim H, Kim N, Jung S, et al. Improvement in skin wrinkles from the use of photostable retinyl retinoate: a randomized controlled trial. *Br J Dermatol*. 2010;162(3):497–502. doi:10.1111/j.1365-2133.2009.09483.x
17. Varani J, Fligiel H, Zhang J, et al. Separation of retinoid-induced epidermal and dermal thickening from skin irritation. *Arch Dermatol Res*. 2003;295(6):255–262. doi:10.1007/s00403-003-0416-5
18. Kurlandsky SB, Duell EA, Kang S, Voorhees JJ, Fisher GJ. Auto-regulation of retinoic acid biosynthesis through regulation of retinol esterification in human keratinocytes. *J Biol Chem*. 1996;271(26):15346–15352. doi:10.1074/jbc.271.26.15346
19. Pople PV, Singh KK. Development and evaluation of topical formulation containing solid lipid nanoparticles of vitamin A. *Aaps Pharmscitech*. 2006;7(4):E63–E69. doi:10.1208/pt070491
20. Abdellatif A, Abou-Taleb HA. Optimization of nano-emulsion formulations for certain emollient effect. *J Pharm Pharm Sci*. 2015;4(12):1314–1328.
21. Dayan N, Touitou E. Carriers for skin delivery of trihexyphenidyl HCl: ethosomes vs. liposomes. *Biomaterials*. 2000;21(18):1879–1885. doi:10.1016/S0142-9612(00)00063-6

22. Paolino D, Lucania G, Mardente D, Alhaique F, Fresta M. Ethosomes for skin delivery of ammonium glycyrrhizinate: in vitro percutaneous permeation through human skin and in vivo anti-inflammatory activity on human volunteers. *J Control Release*. 2005;106(1–2):99–110. doi:10.1016/j.jconrel.2005.04.007
23. David SRN, Hui MS, Pin CF, Ci FY, Rajabalaya R. Formulation and in vitro evaluation of ethosomes as vesicular carrier for enhanced topical delivery of isotretinoin. *Int J Drug Deliv*. 2013;5(1):28.
24. Touitou E, Dayan N, Bergelson L, Godin B, Eliaz M. Ethosomes—novel vesicular carriers for enhanced delivery: characterization and skin penetration properties. *J Control Release*. 2000;65(3):403–418. doi:10.1016/S0168-3659(99)00222-9
25. Meng S, Chen Z, Yang L, et al. Enhanced transdermal bioavailability of testosterone propionate via surfactant-modified ethosomes. *Int J Nanomedicine*. 2013;8:3051. doi:10.2147/IJN.S46748
26. Salem HF, Kharshoum RM, Abou-Taleb HA, Naguib DM. Nanosized nasal emulgel of resveratrol: preparation, optimization, in vitro evaluation and in vivo pharmacokinetic study. *Drug Dev Ind Pharm*. 2019;45(10):1624–1634. doi:10.1080/03639045.2019.1648500
27. Gardouh A, Abou-Taleb H, Solyman S. Preparation, characterization and evaluation of antifungal activity of clotrimazole nanostructured lipid carriers.
28. Elkomy MH, El Menshawe SF, Abou-Taleb HA, Elkarmalawy MH. Loratadine bioavailability via buccal transferosomal gel: formulation, statistical optimization, in vitro/in vivo characterization, and pharmacokinetics in human volunteers. *Drug Deliv*. 2017;24(1):781–791. doi:10.1080/10717544.2017.1321061
29. Ahmed TA. Preparation of transfersomes encapsulating sildenafil aimed for transdermal drug delivery: Plackett–Burman design and characterization. *J Liposome Res*. 2015;25(1):1–10. doi:10.3109/08982104.2014.950276
30. Sarwa KK, Mazumder B, Rudrapal M, Verma VK. Potential of capsaicin-loaded transfersomes in arthritic rats. *Drug Deliv*. 2015;22(5):638–646. doi:10.3109/10717544.2013.871601
31. Elgindy NA, Mehanna MM, Mohyeldin SM. Self-assembled nano-architecture liquid crystalline particles as a promising carrier for progesterone transdermal delivery. *Int J Pharm*. 2016;501(1–-2):167–179. doi:10.1016/j.ijpharm.2016.01.049
32. Rahman SA, Abdelmalak NS, Badawi A, Elbayoumy T, Sabry N, Ramly AE. Formulation of tretinoin-loaded topical proniosomes for treatment of acne: in-vitro characterization, skin irritation test and comparative clinical study. *Drug Deliv*. 2015;22(6):731–739. doi:10.3109/10717544.2014.896428
33. Chourasia MK, Kang L, Chan SY. Nanosized ethosomes bearing ketoprofen for improved transdermal delivery. *Results Pharma Sci*. 2011;1(1):60–67. doi:10.1016/j.rinphs.2011.10.002
34. Higuchi T. Theoretical analysis of rate of release of solid drugs dispersed in solid matrices. *J Pharm Sci*. 1963;52(12):1145–1149. doi:10.1002/jps.2600521210
35. Aboud HM, Ali AA, El Menshawe SF, Elbary AA, Abd elbary A. Development, optimization, and evaluation of carvedilol-loaded solid lipid nanoparticles for intranasal drug delivery. *AAPS Pharmscitech*. 2016;17(6):1353–1365. doi:10.1208/s12249-015-0440-8
36. Abou-Taleb HA, Khallaf RA, Abdel-Aleem JA. Intranasal niosomes of nefopam with improved bioavailability: preparation, optimization, and in-vivo evaluation. *Drug Des Devel Ther*. 2018;12:3501. doi:10.2147/DDDT.S177746
37. Salem HF, Kharshoum RM, Abou-Taleb HA, Naguib DM. Nanosized transferosome-based intranasal in situ gel for brain targeting of resveratrol: formulation, optimization, in vitro evaluation, and in vivo pharmacokinetic study. *AAPS PharmSciTech*. 2019;20(5):181. doi:10.1208/s12249-019-1353-8
38. Moawad FA, Ali AA, Salem HF. Nanotransfersomes-loaded thermosensitive in situ gel as a rectal delivery system of tizanidine HCl: preparation, in vitro and in vivo performance. *Drug Deliv*. 2017;24(1):252–260. doi:10.1080/10717544.2016.1245369
39. Gabal YM, Kamel AO, Sammour OA, Elshafeey AH. Effect of surface charge on the brain delivery of nanostructured lipid carriers in situ gels via the nasal route. *Int J Pharm*. 2014;473(1–2):442–457. doi:10.1016/j.ijpharm.2014.07.025
40. Bancroft JD, Gamble M. *Theory and Practice of Histological Techniques*. Elsevier health sciences; 2008.
41. Saker AA, El-Moez KA, Mohammad RW, Ismail NA. Evaluation of psychiatric morbidity and quality of life in patients with acne vulgaris. *Egypt J Psychiatry*. 2015;36(3):144. doi:10.4103/1110-1105.166357
42. Ahmad A, Alkharfy KM, Wani TA, Raish M. Application of Box–Behnken design for ultrasonic-assisted extraction of polysaccharides from Paeonia emodi. *Int J Biol Macromol*. 2015;72:990–997. doi:10.1016/j.ijbiomac.2014.10.011
43. Li J-C, Zhu N, Zhu J-X, et al. Self-assembled cubic liquid crystalline nanoparticles for transdermal delivery of paeonol. *Med Sci Monit*. 2015;21:3298. doi:10.12659/MSM.894484
44. Annadurai G, Ling LY, Lee J-F. Statistical optimization of medium components and growth conditions by response surface methodology to enhance phenol degradation by Pseudomonas putida. *J Hazard Mater*. 2008;151(1):171–178. doi:10.1016/j.jhazmat.2007.05.061
45. Chandra A, Aggarwal G, Manchanda S, Narula A. Development of topical gel of methotrexate incorporated ethosomes and salicylic acid for the treatment of psoriasis. *Pharm Nanotechnol*. 2019;7(5):362–374. doi:10.2174/2211738507666190906123643
46. Zhang J-P, Wei Y-H, Zhou Y, Li Y-Q, Wu X-A. Ethosomes, binary ethosomes and transfersomes of terbinafine hydrochloride: a Comparative Study. *Arch Pharm Res*. 2012;35(1):109–117. doi:10.1007/s12272-012-0112-0
47. El-Menshawe SF, Ali AA, Halawa AA, El-Din ASS. A novel transdermal nanoethosomal gel of betahistine dihydrochloride for weight gain control: in-vitro and in-vivo characterization. *Drug Des Devel Ther*. 2017;11:3377. doi:10.2147/DDDT.S144652
48. Ahad A, Aqil M, Kohli K, Sultana Y, Mujeeb M. Enhanced transdermal delivery of an anti-hypertensive agent via nanoethosomes: statistical optimization, characterization and pharmacokinetic assessment. *Int J Pharm*. 2013;443(1–2):26–38. doi:10.1016/j.ijpharm.2013.01.011
49. Ahad A, Raish M, Al-Mohizea AM, Al-Jenoobi FI, Alam MA. Enhanced anti-inflammatory activity of carbopol loaded meloxicam nanoethosomes gel. *Int J Biol Macromol*. 2014;67:99–104. doi:10.1016/j.ijbiomac.2014.03.011
50. Ahad A, Aqil M, Kohli K, Sultana Y, Mujeeb M, Ali A. Formulation and optimization of nanotransfersomes using experimental design technique for accentuated transdermal delivery of valsartan. *Nanomedicine*. 2012;8(2):237–249. doi:10.1016/j.nano.2011.06.004
51. Jain S, Patel N, Madan P, Lin S. Quality by design approach for formulation, evaluation and statistical optimization of diclofenac-loaded ethosomes via transdermal route. *Pharm Dev Technol*. 2015;20(4):473–489. doi:10.3109/10837450.2014.882939
52. Lopez-Pinto J, Gonzalez-Rodriguez M, Rabasco A. Effect of cholesterol and ethanol on dermal delivery from DPPC liposomes. *Int J Pharm*. 2005;298(1):1–12. doi:10.1016/j.ijpharm.2005.02.021
53. Salem HF, Kharshoum RM, Abou-Taleb HA, AbouTaleb HA, AbouElhassan KM. Progesterone-loaded nanosized transethosomes for vaginal permeation enhancement: formulation, statistical optimization, and clinical evaluation in anovulatory polycystic ovary syndrome. *J Liposome Res*. 2019;29(2):183–194. doi:10.1080/08982104.2018.1524483
54. Salem HF, El-Menshawe SF, Khallaf RA, Rabea YK. A novel transdermal nanoethosomal gel of lercanidipine HCl for treatment of hypertension: optimization using Box-Benkhen design, in vitro and in vivo characterization. *Drug Deliv Transl Res*. 2020;10(1):227–240. doi:10.1007/s13346-019-00676-5
55. Nagadevi B, Kumar KS, Venkanna P, Prabhakar D. Formulation and characterisation of tizanidine hydrochloride loaded ethosomes patch. *Int J Pharm Pharm Sci*. 2014;6(4):199–205.

56. Hamzawy MA, Abo-youssef AM, Salem HF, Mohammed SA. Antitumor activity of intratracheal inhalation of temozolomide (T. M.Z.) loaded into gold nanoparticles and/or liposomes against urethane-induced lung cancer in BALB/c mice. *Drug Deliv*. 2017;24(1):599–607. doi:10.1080/10717544.2016.1247924
57. Das S, Chaudhury A. Recent advances in lipid nanoparticle formulations with solid matrix for oral drug delivery. *Aaps Pharmscitech*. 2011;12(1):62–76. doi:10.1208/s12249-010-9563-0
58. Garcia-Manyes S, Oncins G, Sanz F. Effect of pH and ionic strength on phospholipid nanomechanics and on deposition process onto hydrophilic surfaces measured by A.F.M. *Electrochim Acta*. 2006;51(24):5029–5036. doi:10.1016/j.electacta.2006.03.062
59. Mohammed MI, Makky AM, Abdellatif MM. Formulation and characterization of ethosomes bearing vancomycin hydrochloride for transdermal delivery. *Int J Pharm Pharm Sci*. 2014;6(11):190–194.
60. Shelke S, Shahi S, Jalalpure S, Dhamecha D. Poloxamer 407-based intranasal thermoreversible gel of zolmitriptan-loaded nanoethosomes: formulation, optimization, evaluation and permeation studies. *J Liposome Res*. 2016;26(4):313–323. doi:10.3109/08982104.2015.1132232
61. Lai F, Pireddu R, Corrias F, et al. Nanosuspension improves tretinoin photostability and delivery to the skin. *Int J Pharm*. 2013;458(1):104–109. doi:10.1016/j.ijpharm.2013.10.007
62. Salem HF, Kharshoum RM, Sayed OM, Abdel Hakim LF. Formulation design and optimization of novel soft glycerosomes for enhanced topical delivery of celecoxib and cupferron by Box–Behnken statistical design. *Drug Dev Ind Pharm*. 2018;44(11):1871–1884. doi:10.1080/03639045.2018.1504963
63. Goindi S, Dhatt B, Kaur A. Ethosomes-based topical delivery system of antihistaminic drug for treatment of skin allergies. *J Microencapsul*. 2014;31(7):716–724. doi:10.3109/02652048.2014.918667
64. Elmoslemany RM, Abdallah OY, El-Khordagui LK, Khalafallah NM. Propylene glycol liposomes as a topical delivery system for miconazole nitrate: comparison with conventional liposomes. *AAPS PharmSciTech*. 2012;13(2):723–731. doi:10.1208/s12249-012-9783-6
65. El-Menshawe SF, Sayed OM, Abou-Taleb HA, El Tellawy N. Skin permeation enhancement of nicotinamide through using fluidization and deformability of positively charged ethosomal vesicles: a new approach for treatment of atopic eczema. *J Drug Deliv Sci Technol*. 2019;52:687–701. doi:10.1016/j.jddst.2019.05.038
66. Shaji J, Lal M. Preparation, optimization and evaluation of transferosomal formulation for enhanced transdermal delivery of a COX-2 inhibitor. *Int J Pharm Pharm Sci*. 2014;6(1):467–477.
67. Sayed OM, El-Ela FIA, Kharshoum RM, Salem HF, Salem HF. Treatment of basal cell carcinoma via binary ethosomes of vismodegib: in vitro and in vivo studies. *AAPS PharmSciTech*. 2020;21(2):51. doi:10.1208/s12249-019-1574-x
68. Salem HF, Nafady MM, Kharshoum RM, Abd el-Ghafar OA, Farouk HO. Mitigation of rheumatic arthritis in a rat model via transdermal delivery of dapoxetine HCl amalgamated as a nanoplatform: in vitro and in vivo assessment. *Int J Nanomedicine*. 2020;15:1517. doi:10.2147/IJN.S238709
69. Zahid SR, Upmanyu N, Dangi S, Ray SK, Jain P, Parkhe G. Ethosome: a novel vesicular carrier for transdermal drug delivery. *J Drug Deliv Ther*. 2018;8(6):318–326. doi:10.22270/jddt.v8i6.2028
70. Arora D, Nanda S. Quality by design driven development of resveratrol loaded ethosomal hydrogel for improved dermatological benefits via enhanced skin permeation and retention. *Int J Pharm*. 2019;567:118448. doi:10.1016/j.ijpharm.2019.118448
71. Faisal W, Soliman GM, Hamdan AM. Enhanced skin deposition and delivery of voriconazole using ethosomal preparations. *J Liposome Res*. 2018;28(1):14–21. doi:10.1080/08982104.2016.1239636
72. Barupal A, Gupta V, Ramteke S. Preparation and characterization of ethosomes for topical delivery of aceclofenac. *Indian J Pharm Sci*. 2010;72(5):582. doi:10.4103/0250-474X.78524
73. Kumar sarwa K, Suresh K, Debnath M, Ahmad M. Tamoxifen citrate loaded ethosomes for transdermal drug delivery system: preparation and characterization. *Curr Drug Deliv*. 2013;10(4):466–476. doi:10.2174/1567201811310040011
74. Abdelbary A, Salem HF, Khallaf RA, Ali AM. Mucoadhesive niosomal in situ gel for ocular tissue targeting: in vitro and in vivo evaluation of lomefloxacin hydrochloride. *Pharm Dev Technol*. 2017;22(3):409–417. doi:10.1080/10837450.2016.1219916
75. Varges R, M. Costa C, S. Fonseca B, F. Naccache M, De Souza Mendes P. Rheological characterization of Carbopol® dispersions in water and in water/glycerol solutions. *Fluids*. 2019;4(1):3. doi:10.3390/fluids4010003
76. Dey S, Mazumder B, Patel J. Enhanced percutaneous permeability of acyclovir by DMSO from topical gel formulation. *Int J Pharm Sci Res*. 2009;1:13–18.
77. Panigrahi L, Ghosal S, Pattnaik S, Maharana L, Barik B. Effect of permeation enhancers on the release and permeation kinetics of lincomycin hydrochloride gel formulations through mouse skin. *Indian J Pharm Sci*. 2006;68(2):2. doi:10.4103/0250-474X.25716
78. Salem HF, Nafady MM, Kharshoum RM, Abd el-Ghafar OA, Farouk HO. Novel enhanced therapeutic efficacy of dapoxetine HCl by nano-vesicle transdermal gel for treatment of carrageenan-induced rat paw edema. *AAPS PharmSciTech*. 2020;21(3):1–13. doi:10.1208/s12249-020-01656-6
79. El-Menshawe SF, Ali AA, Rabeh MA, Khalil NM. Nanosized soy phytosome-based thermogel as topical anti-obesity formulation: an approach for acceptable level of evidence of an effective novel herbal weight loss product. *Int J Nanomedicine*. 2018;13:307. doi:10.2147/IJN.S153429
80. Williams AC, Barry BW. Penetration enhancers. *Adv Drug Deliv Rev*. 2012;64:128–137. doi:10.1016/j.addr.2012.09.032
81. Malakar J, Sen SO, Nayak AK, Sen KK. Formulation, optimization and evaluation of transferosomal gel for transdermal insulin delivery. *Saudi Pharm J*. 2012;20(4):355–363. doi:10.1016/j.jsps.2012.02.001
82. Majithiya RJ, Ghosh PK, Umrethia ML, Murthy RS. Thermoreversible-mucoadhesive gel for nasal delivery of sumatriptan. *AAPS Pharmscitech*. 2006;7(3):E80–E86. doi:10.1208/pt070367
83. John MS, Nair SC, Anoop K. Thermoreversible mucoadhesive gel for nasal delivery of antihypertensive drug. *Int J Pharm Sci Rev Res*. 2013;21(1):57–63.
84. Singh RM, Kumar A, Pathak K. Thermally triggered mucoadhesive in situ gel of loratadine: β-cyclodextrin complex for nasal delivery. *AAPS PharmSciTech*. 2013;14(1):412–424. doi:10.1208/s12249-013-9921-9
85. Rahman SA, Abdelmalak NS, Badawi A, Elbayoumy T, Sabry N, El ramly A. Tretinoin-loaded liposomal formulations: from lab to comparative clinical study in acne patients. *Drug Deliv*. 2016;23(4):1184–1193. doi:10.3109/10717544.2015.1041578
86. Sabouri M, Samadi A, Nasrollahi SA, et al. Tretinoin loaded nanoemulsion for acne vulgaris: fabrication, physicochemical and clinical efficacy assessments. *Skin Pharmacol Physiol*. 2018;31(6):316–323. doi:10.1159/000488993
87. Lucky AW, Sugarman J. Comparison of micronized tretinoin gel 0.05% and tretinoin gel microsphere 0.1% in young adolescents with acne: a post hoc analysis of efficacy and tolerability data. *Cutis*. 2011;87(6):305–310.
88. Torok HM, Pillai R. Safety and efficacy of micronized tretinoin gel (0.05%) in treating adolescent acne. *J Drugs Dermatol*. 2011;10(6):647–652.
89. Webster G, Cargill DI, Quiring J, Vogelson CT, Slade HB. A combined analysis of 2 randomized clinical studies of tretinoin gel 0.05% for the treatment of acne. *Cutis*. 2009;83(3):146–154.